AD NUMBER

ADB010635

LIMITATION CHANGES

TO:

Approved for public release; distribution is unlimited.

FROM:

Distribution authorized to U.S. Gov't. agencies only; Test and Evaluation; MAR 1975. Other requests shall be referred to Air Force Avionics Laboratory, Attn: AFAL/DHO, Wright-Patterson AFB, OH 45433.

AUTHORITY

WL/AFSC ltr, 12 Apr 1991

AFAL-TR-75-64
Part II

Er:YLF LASER DEVELOPMENT
Part II Advanced Research Projects Agency

Sanders Associates, Inc.
95 Canal Street
Nashua, New Hampshire 03060

March 1976

TECHNICAL REPORT AFAL-TR-75-64, PART II
Final Report for Period 1 November 1974 - 10 July 1975

AIR FORCE AVIONICS LABORATORY
AIR FORCE WRIGHT AERONAUTICAL LABORATORIES
AIR FORCE SYSTEMS COMMAND
WRIGHT-PATTERSON AIR FORCE BASE, OHIO 45433

NOTICE

When Government drawings, specifications, or other data are used for any purpose other than in connection with a definitely related Government procurement operation, the United States Government thereby incurs no responsibility nor any obligation whatsoever; and the fact that the government may have formulated, furnished, or in any way supplied the said drawings, specifications, or other data, is not to be regarded by implication or otherwise as in any manner licensing the holder or any other person or corporation, or conveying any rights or permission to manufacture, use, or sell any patented invention that may in any way be related thereto.

Distribution limited to U.S. Government agencies only; test and evaluation results reported; March 1975. Other requests for this document must be referred to the Air Force Avionics Laboratory (AFAL/DHO), Wright-Patterson AFB, Ohio 45433.

This technical report has been reviewed and is approved for publication.

Richard L Remski

RICHARD L. REMSKI
Project Engineer

FOR THE COMMANDER

William A. Wallace

WILLIAM A. WALLACE, Major, USAF
Acting Chief
Electro-Optics Technology Branch

AIR FORCE - 19 APRIL 1976 - 125

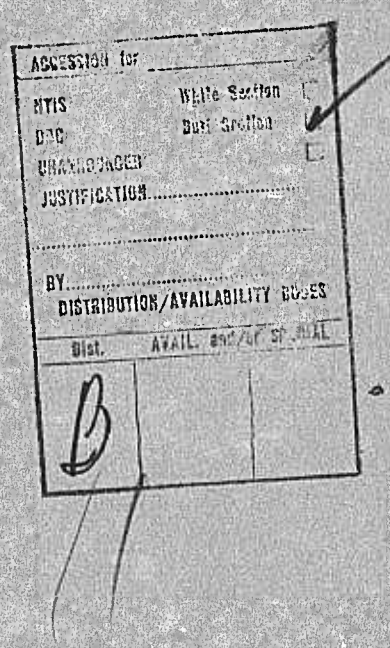

SECURITY CLASSIFICATION OF THIS PAGE *(When Date Entered)*

REPORT DOCUMENTATION PAGE

READ INSTRUCTIONS BEFORE COMPLETING FORM

1. REPORT NUMBER: AFAL-TR-75-64-Pt-2
2. GOVT ACCESSION NO.
3. RECIPIENT'S CATALDG NUMBER

4. TITLE *(and Subtitle)*: Er:YLF Laser Development, Part II.

5. TYPE OF REPORT & PERIDD COVERED: Final Report. 1 Nov 1974 - 10 July 1975

6. PERFORMING ORG. REPORT NUMBER

7. AUTHDR(s): E.P. Chicklis, R.C. Folweiler, J.D. Kuppenheimer, C.S. Naiman, D.R. Gabbe and A. Linz

8. CONTRACT DR GRANT NUMBER(s): F33615-74-C-1194, ARPA Order-2075

9. PERFORMING ORGANIZATION NAME AND AODRESS
Sanders Associates, Inc.
95 Canal St.
Nashua, NH 03060

10. PROGRAM ELEMENT, PROJECT, TASK AREA & WORK UNIT NUMBERS

11. CONTROLLING OFFICE NAME AND ADDRESS
Advanced Research Projects Agency
Materials Science Directorate
1400 Wilson Blvd., Arlington, VA 22209

12. REPORT DATE: November 1975

13. NUMBER OF PAGES: 84

14. MONITORING AGENCY NAME & AOORESS*(if different from Controlling Office)*
AFAL/DHO
Wright-Patterson Air Force Base,
Ohio 45433

15. SECURITY CLASS. *(of this report)*: Unclassified

15a. OECLASSIFICATION/DOWNGRADING SCHEOULE: N/A

16. OISTRIBUTION STATEMENT *(of this Report)*

Distribution limited to U.S. Government agencies only; test and evaluation results reported; March 1975. Other requests for this document must be referred to the Air Force Avionics Laboratory (AFAL/DHO), Wright-Patterson AFB, Ohio 45433.

17. OISTRIBUTION STATEMENT *(of the abstract entered in Block 20, if different from Report)*

N/A

12 98p.

18. SUPPLEMENTARY NDTES

N/A

19. KEY WORDS *(Continue on reverse side if neceeeary and identify by block number)*

0.85 Micron Laser	IR Laser	Optically Pumped Laser
Er:YLF	YLF	Rare Earth Spectroscopy
Erbium Laser	Top Seeded Solution Fluoride Laser Material	Rare Earth Laser
		Erbium

20. ABSTRACT *(Continue on reverse side if necessary and identify by block number)*

Growth and laser performance of the laser material Er:YLF was investigated. This is a 4 level laser emitting at 0.85 microns and operated in the flash pumped mode at room temperature.

Large, uniform diameter boules of Er:YLF have been grown under automatic diameter control in an argon atmosphere. 0.25 x 3 inch rods with scattering (continued)

OVER

DD FORM 1 JAN 73 1473 EDITION OF 1 NOV 65 IS OBSOLETE

UNCLASSIFIED
SECURITY CLASSIFICATION OF THIS PAGE *(When Date Entered)*

20 loss less than 0.5% cm^{-1} and optical path distortion of less than 1 fringe per inch have been routinely grown on this program. The rod yield is limited only by external geometry; there are no cores in this material. Boule uniformity and boule-boule reproducibility was excellent.

Two feed purification procedures were employed in this program. Good results were obtained with hydrofluorination of molten Li YF_4 from commercial YF_3 - ReF_3 - LiF. Further improvement in material quality was demonstrated on one growth run using Y_2O_3 - Re_2O_3 purified by solvent extraction then converted to the fluoride.

Comparative laser testing showed a linear increase in laser efficiency with Er concentration from 2 - 5% Er. At 10 Hz, long pulse, 1.1 watts output were measured from a 0.25 x 3 inch rod with a slope efficiency of 0.5% (overall efficiency 0.3%) at room temperature. At 10 Hz, a 5 x 36mm rod exhibited a measured beam divergence of 1.5 mr at 200 watts input. At this 200 watts input, 0.58 watts output were obtained.

Higher output powers were constrained by flashlamp peak current limitations. Q-switched outputs at 1/2 the long pulse efficiency were obtained.

PREFACE

This is the second semi-annual report on Contract F33615-74-C-1194 covering the work performed to develop the 0.85 micron solid state laser material Erbium:Yttrium Lithium Fluoride. This work is sponsored by the Advanced Research Projects Agency under ARPA Order No. 2075 AMD #3. The inclusive dates of the research reported herein are 1 November 1974 to 10 July 1975. The work on the first part of the program is described in AFAL-TR-75-64 (Part I).

Mr. Richard L. Remski (DHO), Air Force Avionics Lab, Air Force Systems Command, Wright-Patterson Air Force Base, Ohio is the Project Monitor of this program.

These studies were carried out at Sanders Associates, Defensive Systems Division. Dr. C.S. Naiman, Manager - Laser Systems Department is the Project Supervisor and E.P. Chicklis and R.C. Folweiler are the principal investigators. Dr. J.D. Kuppenheimer provided technical support and Mr. J.C. Doherty assisted with the laser measurements.

Crystals were grown for this program at the Sanders Associates Automated Fluoride Growth Facility. Investigation of crystal growth phenomena was carried out by Dr. D.R. Gabbe on a subcontracting basis at the Center of Material Sciences and Engineering, Massachusetts Institute of Technology, under the supervision of Dr. A. Linz.

TABLE OF CONTENTS

LIST OF ILLUSTRATIONS

LIST OF ILLUSTRATIONS (Continued)

LIST OF TABLES

1.0 INTRODUCTION

1.1 OBJECTIVE

The objective of this program was to improve the quality and yield of the laser material Er^{3+}:YLF and to define laser performance in the long pulse and Q-switched modes. This work is a continuation of investigations of this material sponsored through ARPA Order No. 2075, begun under Contract F33615-72-C-2065, and reported in AFAL-TR-73-94, Parts I, II and III. The goals of this program were:

- Growth of 0.25 x 3 inch rods with scattering loss $<0.5\%\ cm^{-1}$.
- Operation in the electro-optically Q-switched mode at 10 Hz with output powers in excess of 1 watt, beam divergence less than 5 mr.
- Overall efficiency of 0.5% in the Q-switched mode.

The results of the first six months of this investigation are reported in AFAL-TR-75-64 Part I.

1.2 BACKGROUND

Air Force applications requiring narrow beam near infrared devices for active illumination of targets typically utilize receiver systems with spectral response up to 1 micrometer. Sensitivity of such receivers is generally greatly decreased beyond 0.9 micrometers, and a good operating wavelength regime is between 0.8 and 0.9 micrometers Operation at 0.85 micrometers offers the additional advantage of compatibility with gallium arsenide array/low light level TV systems currently in prototype phases.

Sanders Associates, Inc. in conjunction with the Crystal Physics Laboratory, Department of Electrical Engineering, MIT, demonstrated laser action at $\lambda = 0.85$ μm in Er^{3+}:YLF at room temperature in 1971. Preliminary data (100 joule pulsed threshold 0.1% slope efficienty) in single shot operation led to the first program to develop this material for Air Force illuminator applications. The results of this first program were definition of the thermal and mechanical properties, demonstration of laser operation at up to 50 Hz with measured outputs of up to 0.8 watts, and definition of the laser related spectroscopic parameters. Improved laser efficiency with increasing Er^{3+} concentration was predicted, and the effects of the long lived terminal manifold analyzed and shown to be insignificant for single shot applications.

In 1973 Sanders Associates, Inc., in conjunction with the Crystal Physics Laboratory at MIT, embarked upon a program to transfer the technology of growth of this fluoride host to Sanders Associates. To that end design and construction of a facility for automated growth of fluoride hosts was carried out under company funding. Construction of the furnace was completed in 1974; and the first growth run carried out under this program was completed in September 1974.

1.3 RESULTS

The results obtained in this program are:

- Growth of large YLF boules of uniformly high optical quality has been demonstrated
- Uniformity of the boules (lack of cores) has resulted in a rod yield limited by external geometry
- 0.25 x 3 inch rods with less than 1 fringe per inch path distortion have been routinely obtained

- 0.25 x 3 inch rods with scattering loss less than 0.5% cm^{-1} have been routinely grown

- Improved feed purification procedures have been developed and shown to result in substantially improved material

- The effect of the long lived terminal manifold has been shown to be negligible for repetition rates below about 30 Hz.

- Laser efficiency has been shown to increase linearly with Er^{3+} concentration from 2 - 5% Er, verifying previous predictions

- Laser beam divergence of 1.4 mr has been measured at a loading corresponding to an output of 0.17 watts/cm (0.5 x 3.6 cm active volume).

- Performance comparisons of 0.25 x 3 inch Nd:YAG and 7.5% Er:YLF in the same pump cavity show that Er:YLF exhibits about 1/3 the slope efficiency of Nd:YAG.

- 10Hz long pulse outputs of 1 watt at 0.3% overall (0.5% slope) efficiency have been demonstrated

- Q-switched operation at 1/2 the long pulse efficiency has been demonstrated.

2.0 CRYSTAL GROWTH

All the crystals for this program were grown at the Sanders Associates Automated Fluoride Growth Facility. After the initial seeding, necking and diameter expansion procedures, the entire boules were grown under automated diameter control. The procedures adopted for growth of Er^{3+}:YLF boules have resulted in the reproducible growth of material of uniformly excellent optical quality for this program. In the following parts of this section, the growth technique is very briefly reviewed and the results of the growth runs are described.

2.1 REVIEW OF THE GROWTH TECHNIQUE

Details of the growth technique are described in references 2 and 3. A comprehensive description of the growth chemistry and of the effects of feed purification on material quality are presented in reference 3. YLF crystals are grown at Sanders and MIT in an inert atmosphere of high purity argon from a rigirously clean melt at the growth temperature of approximately 900°C. The growth technique is Top Seeded Solution, which is a modification of the Czochralski process; crystals are pulled at between 1.0 and 1.5 mm per hour. Figures 1 and 2 show photos of the Sanders growth installation.

To eliminate continuous operator attention and assure more uniform growth conditions, crystals are pulled (after the initial seeding) under automated diameter control. Except for the rotation rate, this system controls all parameters of the growth process - pulling rate, temperature lowering rate, crucible lift, and diameter. A block diagram of the system is shown in figure 3. Diameter control is effected by a sensing of the reflection of a He-Ne laser from the meniscus at the crystal/melt interface. A block diagram of the diameter control system is shown in figure 4.

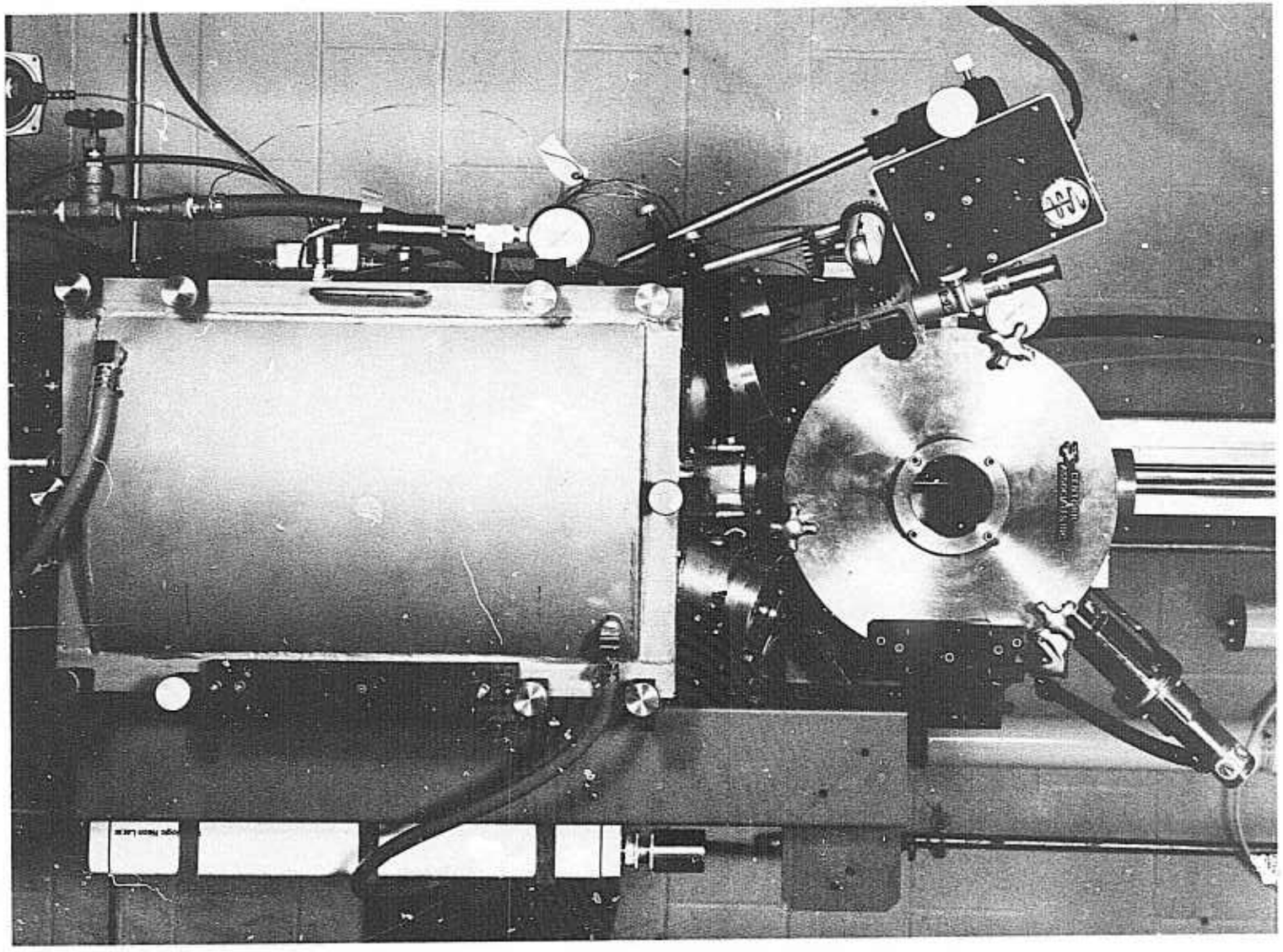

Figure 1. Crystal Growth - Furnace Exterior

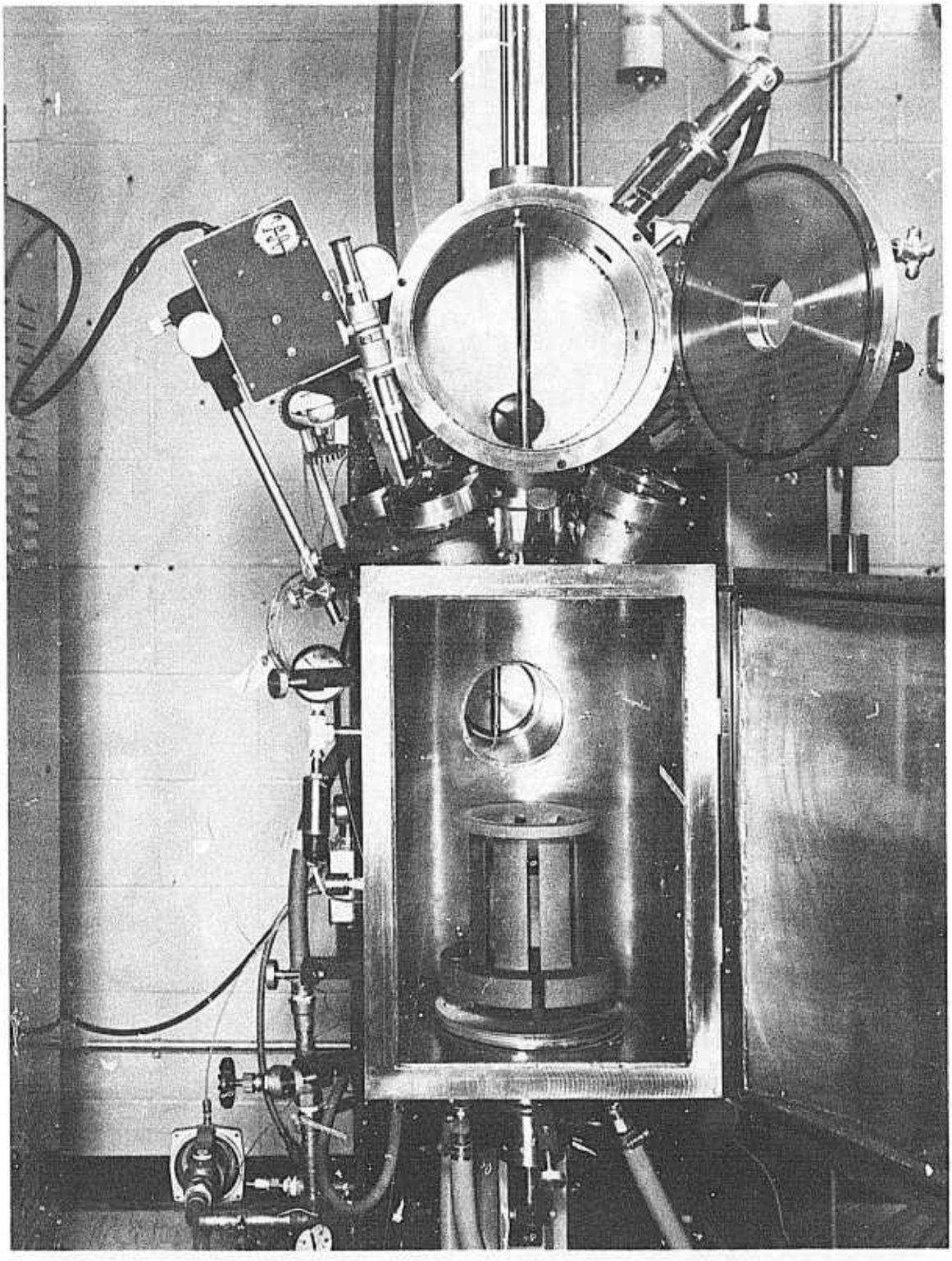

Figure 2. Crystal growth - furnace interior.

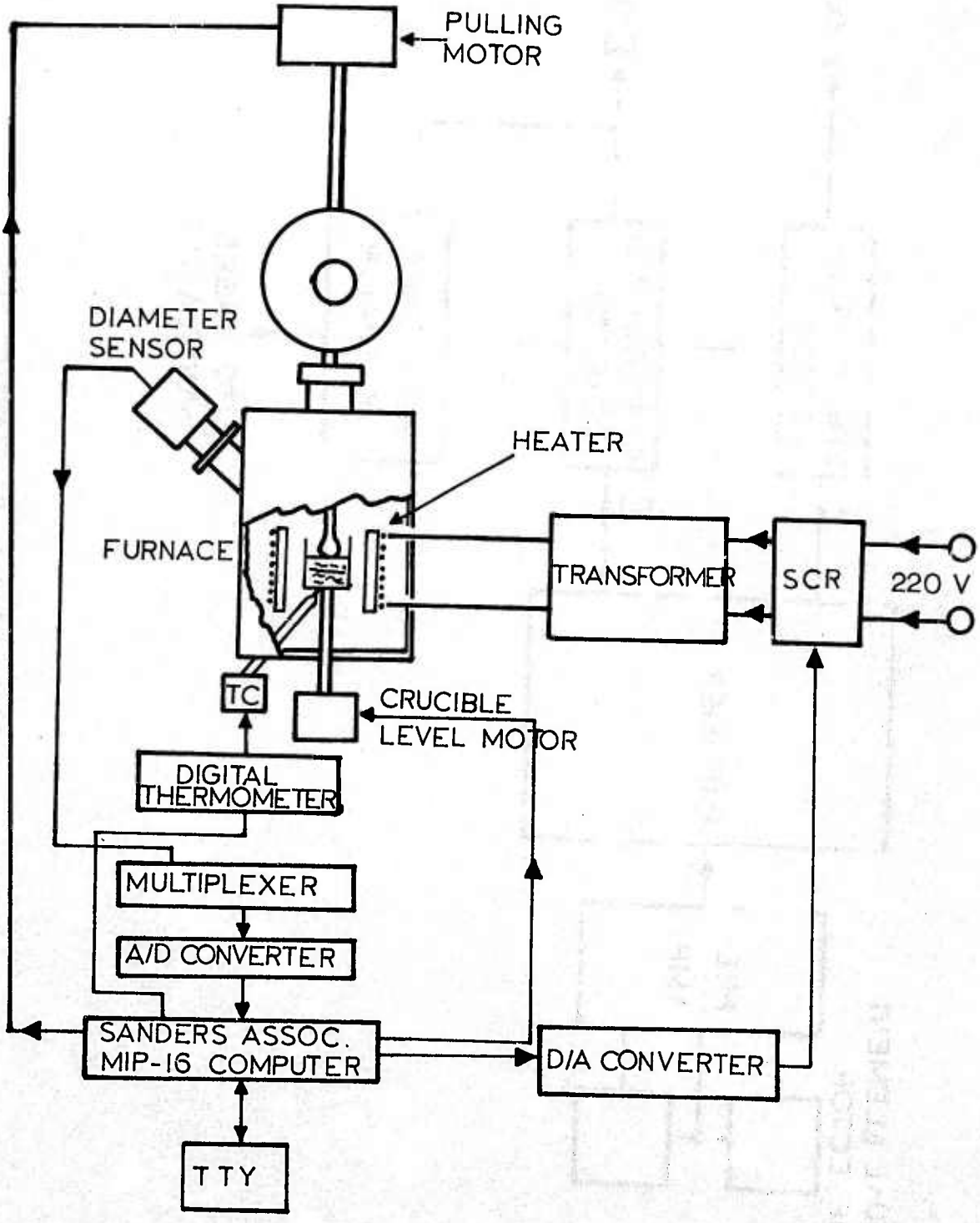

Figure 3. Block diagram of computer control system.

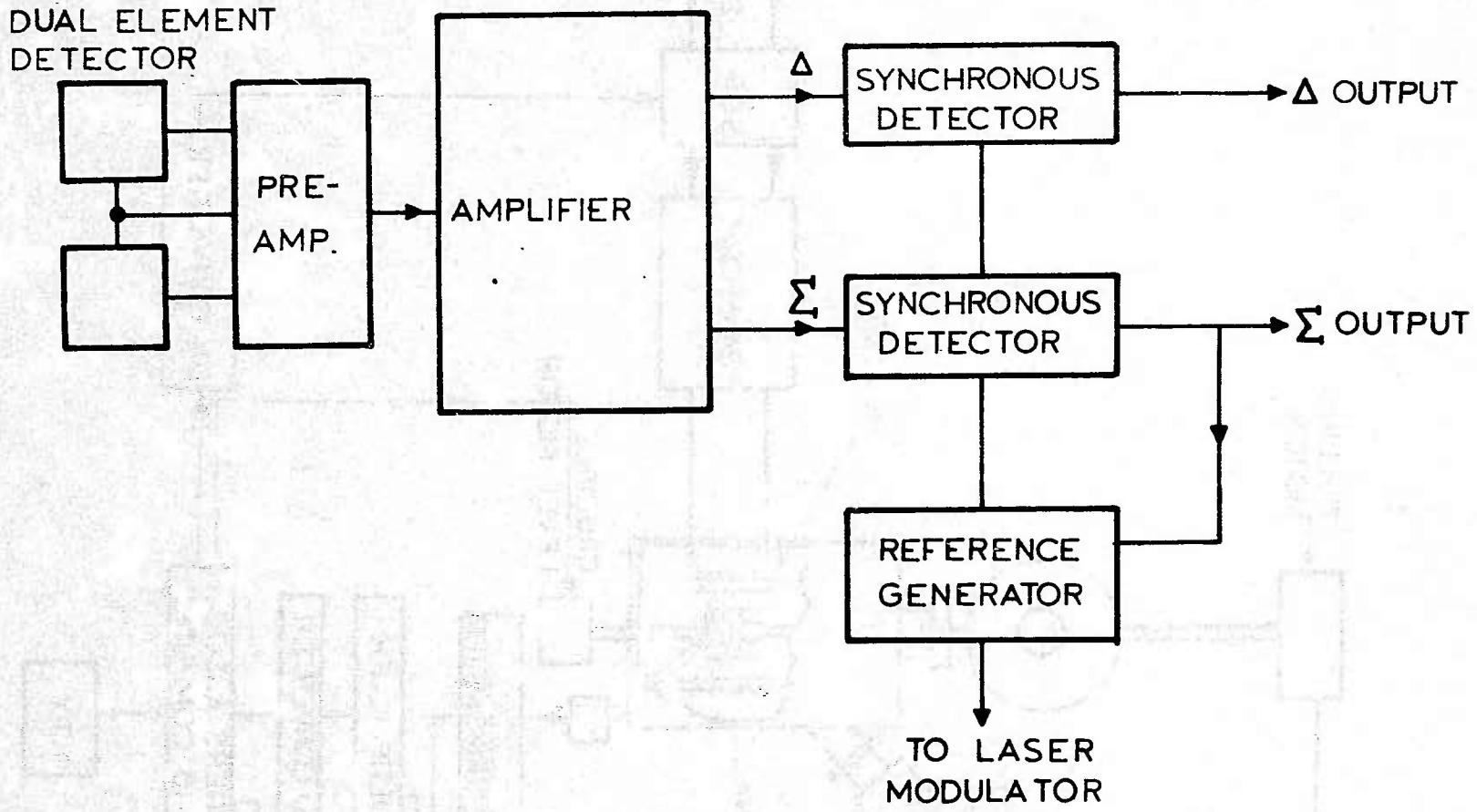

Figure 4. Block diagram of diameter sensor.

2.2 CRYSTALS GROWN

Tables 1 and 2 list all the crystals grown in this program. The details of each growth run together with the resultant crystalline quality described in detail below.

2.2.1 Shake-down Runs

Boules 101 Yc and 103 Yc are shown in figures 5 and 6. Boule 101 Yc was grown without a seed (hence is polycrystalline) under manual control; 103 Yc was grown from a seed under diameter control, but had to be aborted due to an instability in the control loop. A concave surface at the growth interface indicated an undesirable furnace gradient[3]. After this run, the heat shielding of the furnace was modified to increase the furnace gradient. All the rest of the growth runs were seeded.

Boule 104 Y was aborted due to a furnace leak which contaminated the feed. The crystal and remaining charge from 104 Y was rehydrofluorinated and used for the growth of 105 Y. Figure 7 shows the crystal as grown, which became noncircular near the end of the growth. The diameter sensor operated correctly during the growth run. Indications of air leakage during growth were confirmed by analysis of the crystal, viz: YOF was identified by X-ray diffraction analysis. The leak was traced to the seed rod seal which was extensively reworked.

These first four runs identified the problem areas with the furnace and control loop, and at this point the known problems were solved. In addition, the importance of a proper thermal gradient was clearly established by the observed effects of gradient on the crystal shape. More detailed studies of the effects of furnace shielding and rotation rate on the growth interface are presented in the next section of this report.

TABLE 1

Er:YLF GROWTH

Boule No.	Composition	Weight of Charge (gms)	Weight of Boule (gms)	length/ diameter (mm)	Feed	Remarks
101Yc	$LiYF_4$	109	80	80/20	RC*:YF_3 H^+ :LiF	Manual Control No seed
103Yc	$LiYF_4$ 3.5% Er	138	23	38/13	RC:YF_3,ErF_3 H :LiF	Diameter Control Unstable control loop-concave interface
104Yb	$LiYF_4$ 5% Er	260	40		RC:ErF_3 YF_3 H :LiF	Air leak Concave Interface Remelted
105Yb	$LiYF_4$ 5% Er	260	91	95/19	Rehydrofluorinated Melt of 104 Yb	Non-circular cross section
106Yb	$LiYF_4$ 5% Er	169	99	115/17	Same as 105 Yb	Computer Control Extremely straight sides (figure 8)

* RC = Research Chemicals
+H = Harshaw Chips

TABLE 2

Er:YLF GROWTH

Boule No.	Composition	Weight of Charge (gms)	Weight of Boule (gms)	length/ diameter (mm)	Feed	Remarks
107Y	$LiYF_4$ 3.5% Er	299	195	160/21	RC*:YF_3 (6N) RC:ErF_3 (5N) H :LiF	Diameter Control Fig. 10
108Y	$LiYF_4$	328	223	140/24	RC:YF_3 ErF_3 H :LiF	Diameter Control Flat sides (Fig. 12)
109Y	$LiYF_4$ 10% Er	400	~270	170/26	RC Y_2O_3, Er_2O_3 Converted to $RE_2(CO_3)_3$ HF at 300: REF_3 HF at 800 HF at 825 ($LiF + YF_3$)	Clear Surface Furnace failure caused melt to freeze, breaking crystal at seed. (5)0.25 x 3 inch rods cut Fig. 15

* RC = Research Chemicals

H = Harshaw

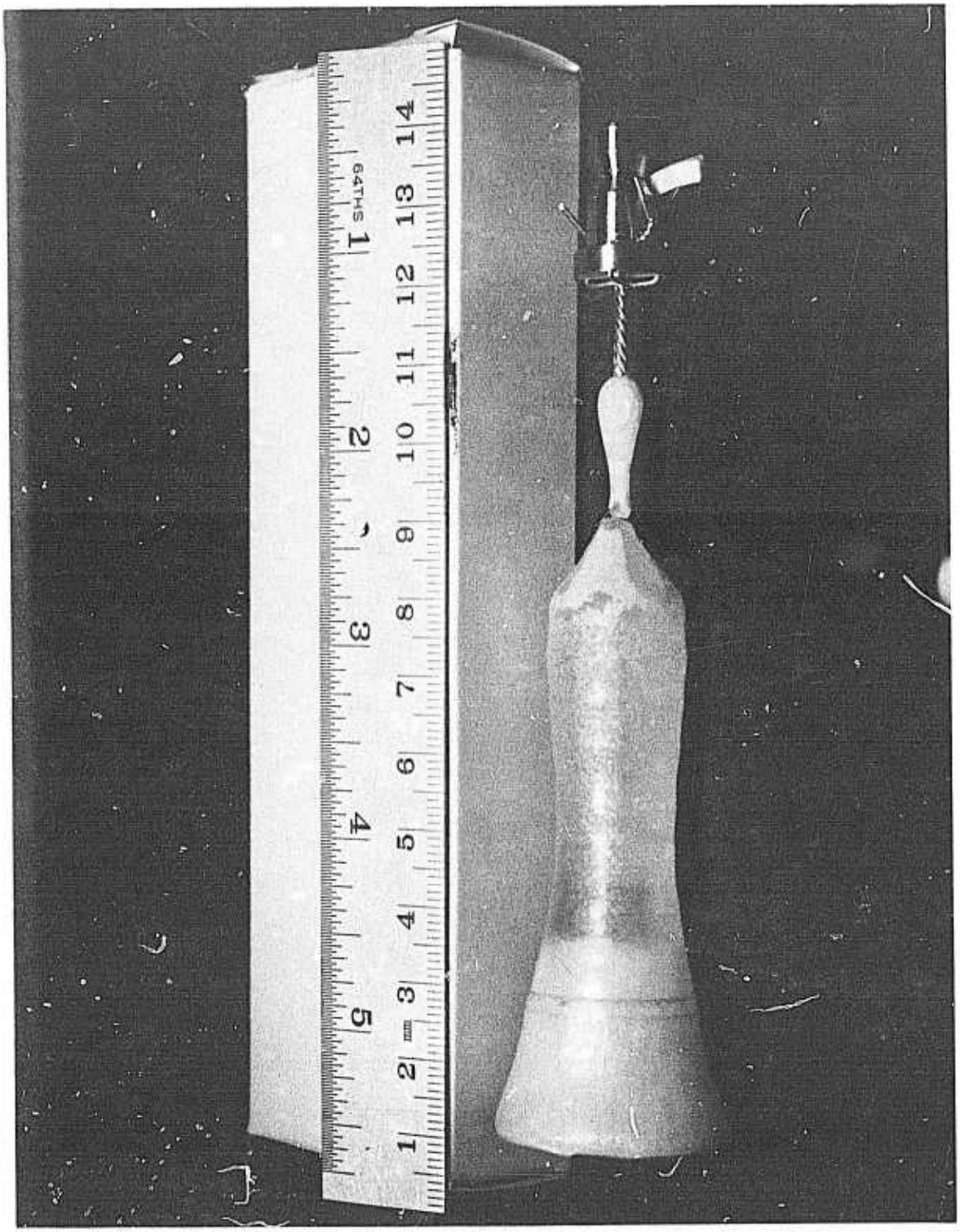

Figure 5. Boule 101 Yc.

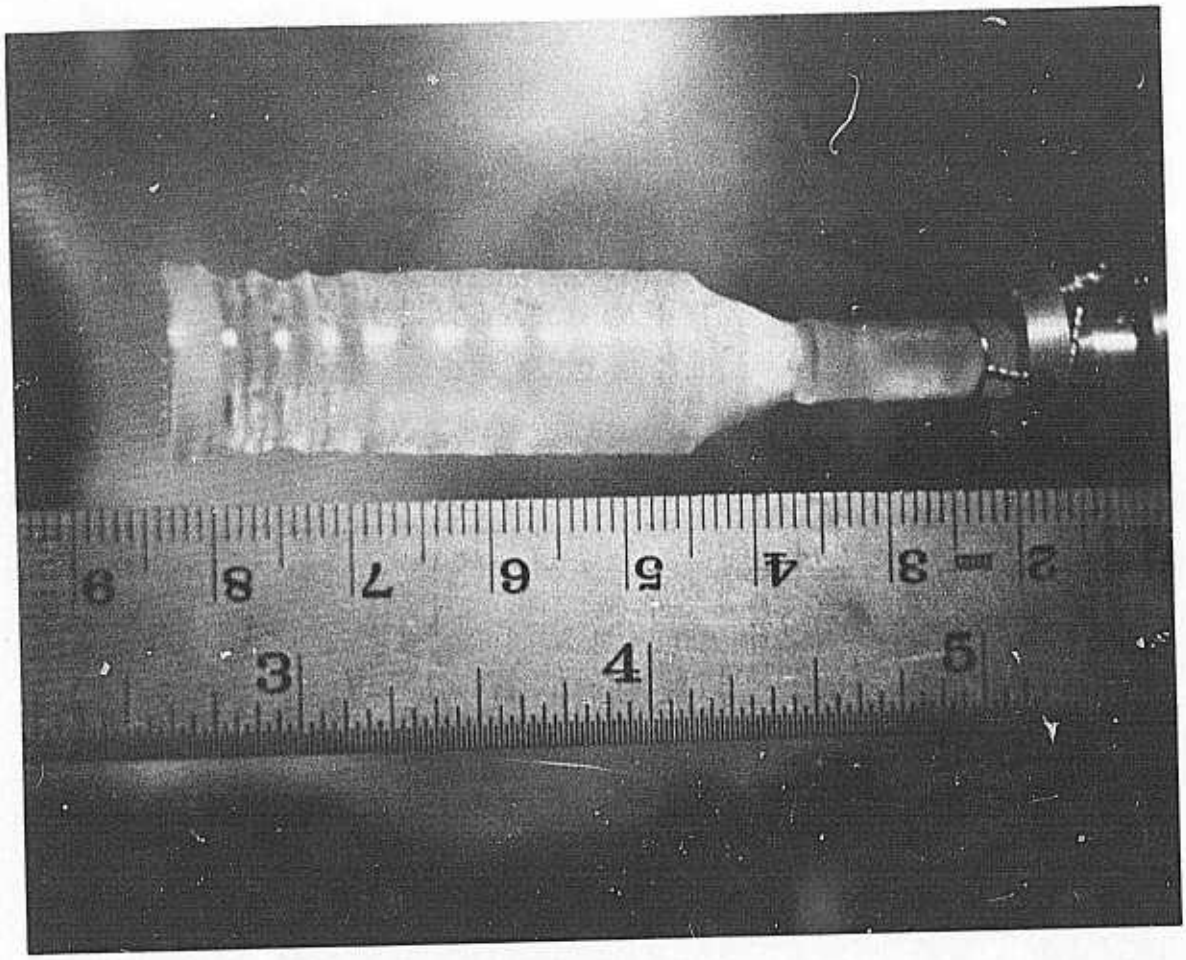

Figure 6. Boule 103 Yc

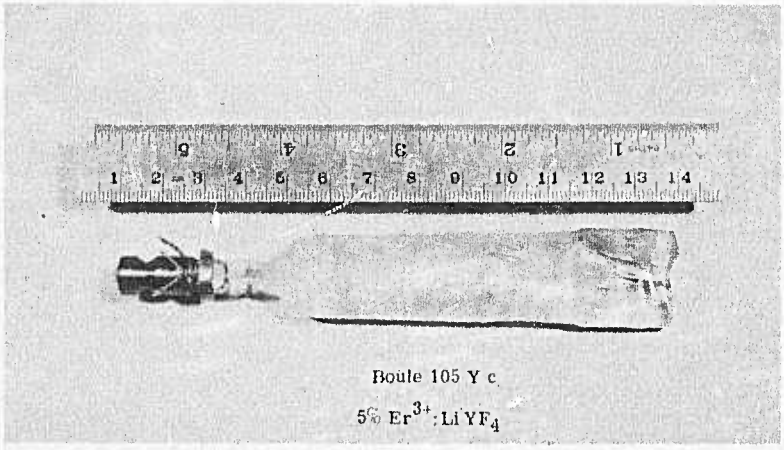

Figure 7. Boule 105 Y c.

2.2.2 Laser Boules

106 Y: The remaining melt from 105 Y was used for the growth of this boule. The thermal gradient was increased and a reworked rod seal eliminated any leaks. In this run, diameter control was used after the crystal was brought to a stable (cylindrical) diameter by manual control. Growth was interrupted by a power failure during which the emergency generator failed to start. As a result, the partially grown crystal became stuck in the frozen melt. The crystal was melted back approximately two millimeters from the frozen interface and growth restarted.

Growth occurred for approximately 9 hours of unattended operation. The resulting boule, shown in figure 8 was 16.7 $\pm$ 0.2 mm in diameter over the central 85 mm. The pulling rate was 1.0 mm/hr; the crucible was raised at 0.1 mm/hr; and the rotation rate was 60 rpm. Interferograms of the rods cut from the boule, shown in figure 9, indicate the very high optical quality of this material. Under a polarizing microscope, however, some low angle grain boundaries were observed with misorientations up to 0.5 degrees at the top and bottom of the boule. The presence of some grains at the top of the boule indicated that the seeding and neck-down operation required further refinement.

107 Y: The seeding for this run was performed in the usual way except that greater care was taken to form and stabilize the neck and to assure a circular cross section at the neck. Careful "neck-down" is important in order to promote good nucleation (i.e., to assure that no randomly nucleated material generated from the initial contact remains on the seed). However, the change in the thermal impedance due to the smaller neck had apparently reduced the gradient at the interface. The crystal was melted back twice without success; i.e., a noncircular growth interface developed. During the third attempt, melt turbulence was observed which was eliminated by lowering the rotation

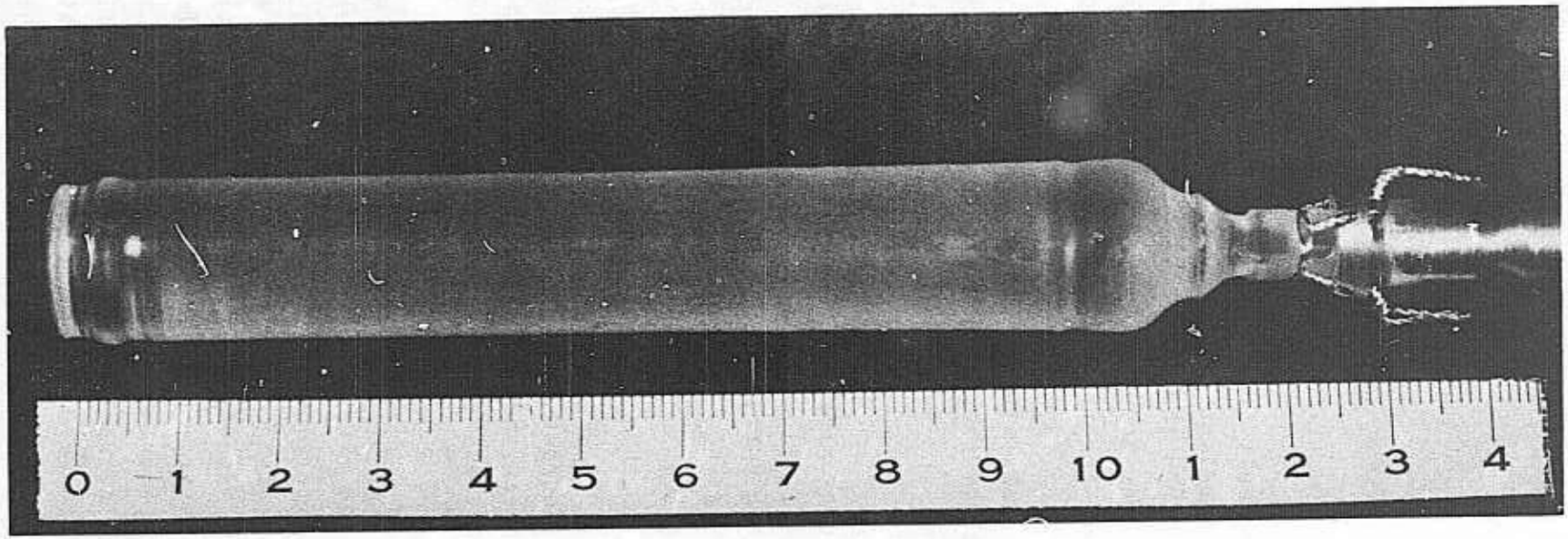

Boule 106 Y b

5% Er^{3+}: Li YF_4

Figure 8. Boule 106 Y b.

LASER ROD INTERFEROGRAMS

BOULE NO. 106Yb

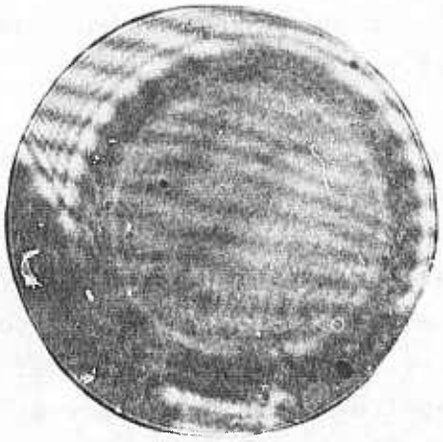

ROD NO. 476.1
1/4"x3"

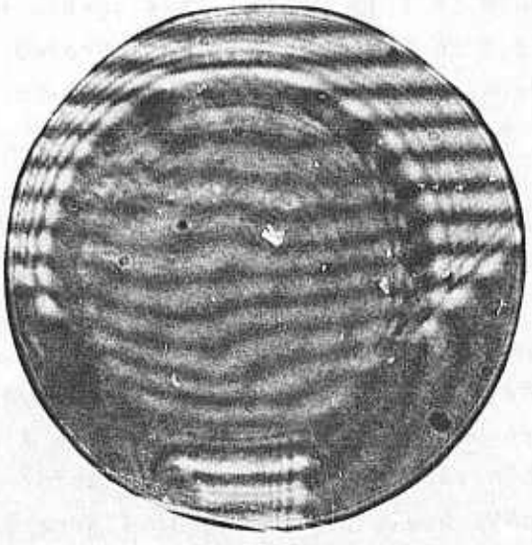

ROD NO. 476.2
1/4"x3"

Figure 9. Laser rod interferograms.

rate from 60 to 25 rpm. At this rotation rate, the concave portions of the cross section began filling in and became nearly circular by the end. The crystal was grown unattended under these conditions for approximately 90 hours.

The resulting boule (107 Yc) weighed 195 gm with the seed, with an overall length greater than 170 mm; the 100 mm long straight walled section at the bottom had a diameter of approximately 20 mm. The boule, shown in Figure 10, had an unusual surface texture. The portion grown at 60 rpm had the hazy, etched surface observed in previous runs; the portion grown at 25 rpm had an appearance similar to flame polished sapphire boules. Laser rods have not been fabricated from this boule, but visual inspection through the polished ends showed that the boule was of high optical quality.

108 Y: The experience of the previous runs was successfully applied to the growth of this boule. A slightly modified thermal gradient was provided to accommodate the improved seeding procedure. Particular care was exercised to obtain a well-shaped neck at the start. The result is shown in Figure 11.

After the neck-down procedure, the entire boule was grown under automated diameter control at a rotation rate of 25 rpm and a pull rate of 1.5 mm/hr. The resulting boule shown in figure 12 was approximately 110 mm long with a diameter between 22 - 30 mm. The boule weight was approximately 223 gms. The optical quality of the boule was quite uniform; three 0.25 x 3 inch, and three 5 x 60 mm, rods were cut with considerable surplus material. Interferograms of some of the rods cut from this boule are shown in figure 13. Near the bottom of the boule some slightly misoriented grains were observed in a polarizing scope. No evidence of grain boundaries was observed in the top part of the boule.

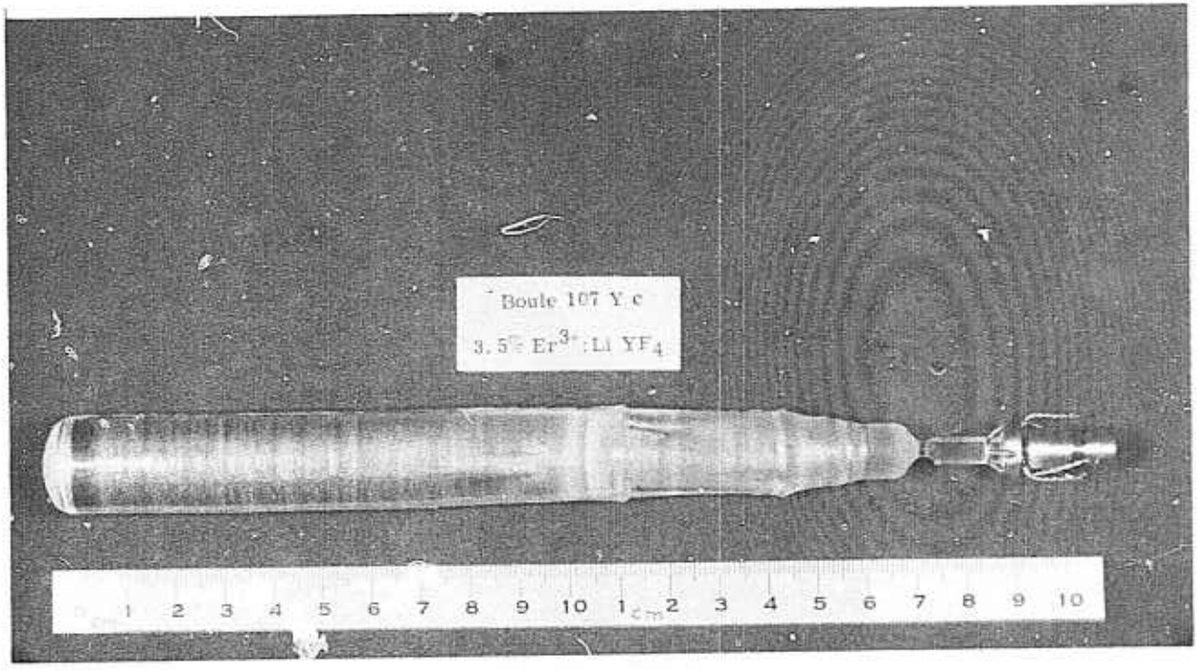

Figure 10. Boule 107 Y c.

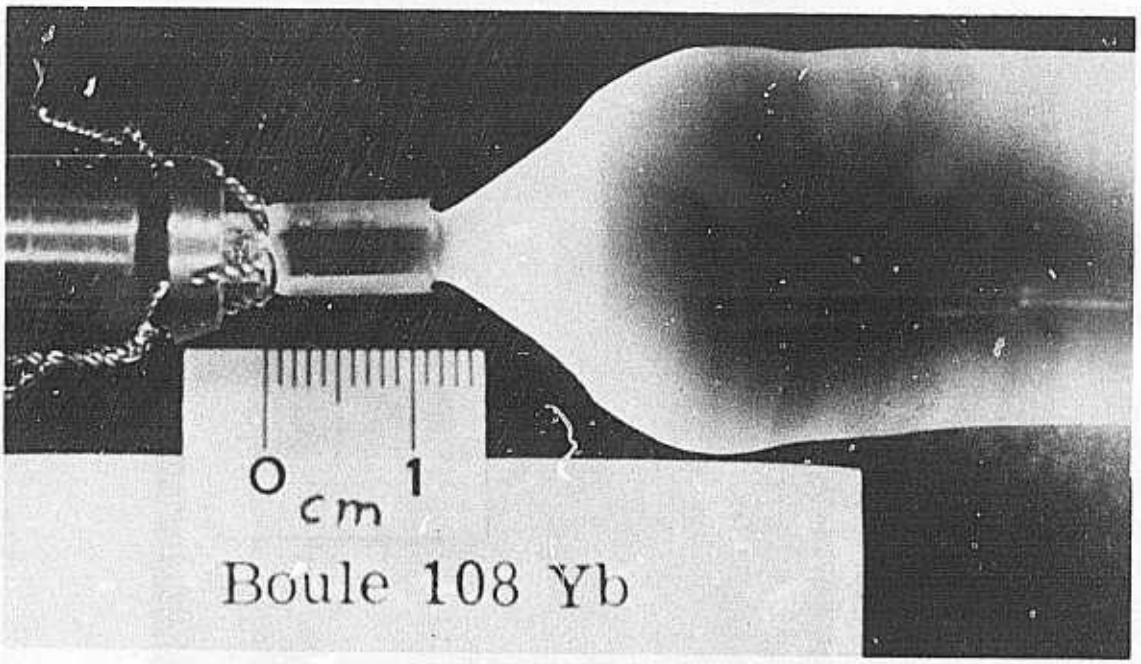

Figure 11. Neck of boule 108 Yb.

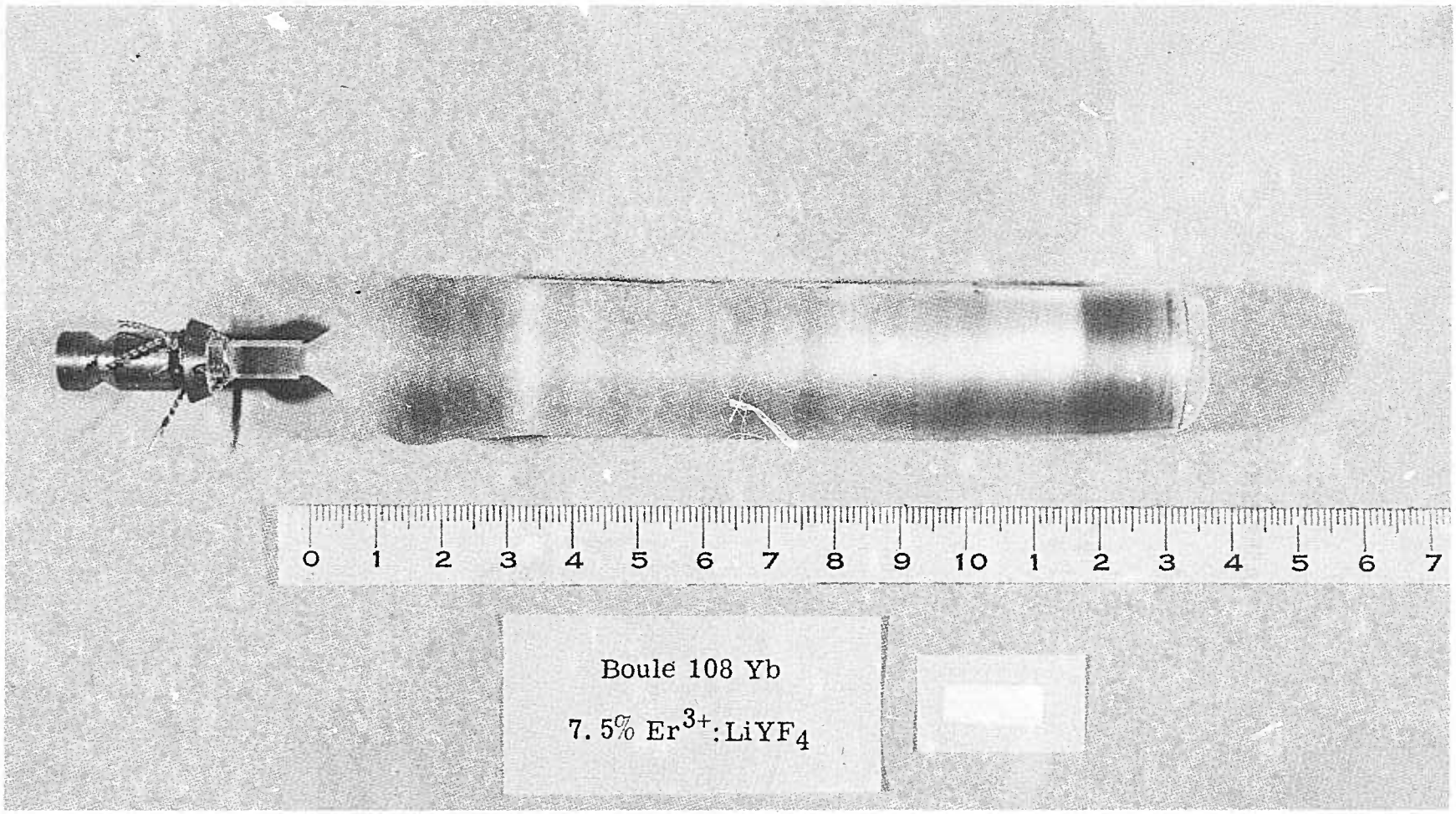

Figure 12. Boule 108 Y b.

LASER ROD INTERFEROGRAMS
BOULE NO. 108Y

ROD NO.479.2
5 mm x 40 mm

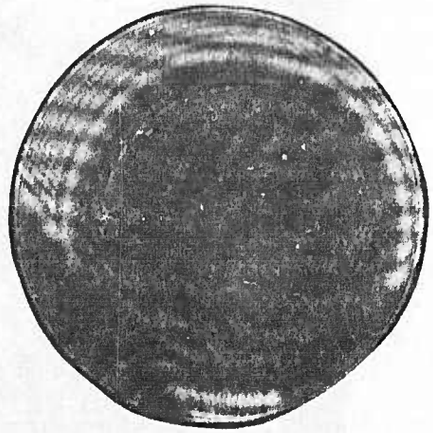

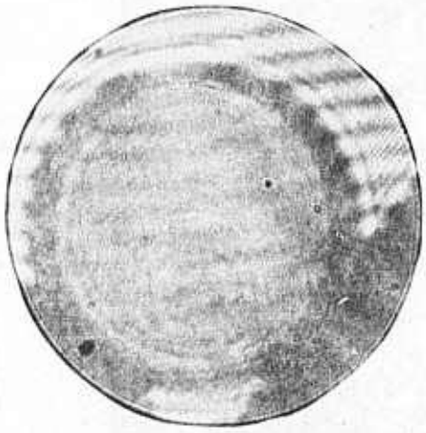

ROD NO. 479.3
0.25"x3"

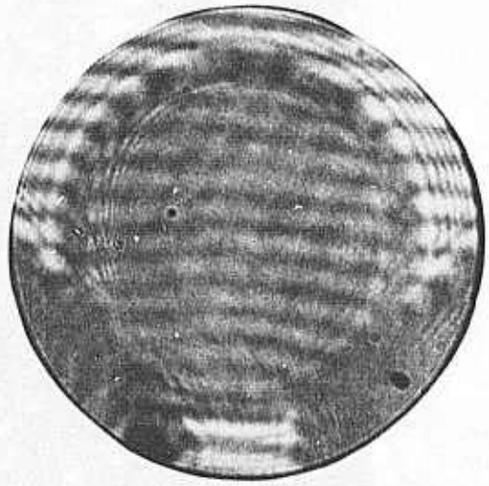

ROD NO. 479.4
0.25"x3"

Figure 13. Laser Rod Interferograms.

109 Y: The feed material for this growth run was synthesized at MIT starting from rare earth oxides. Details of feed purification procedures for this and other growth runs is presented in section 3 of this report. This growth run was of particular interest as it provided an opportunity to compare the effects of feed preparation on the growth and quality of this material.

Prior to the start of the growth run, leaks in the furnace were found at some of the furnace body weld seams. The welds were repaired and the growth initiated under (nominally) the same conditions as in 108 Y.

Figure 14 shows the neck of 109 Y, and in figure 15 the entire boule is shown. The obvious anomaly shown in figure 15 was the result of a power shut-off just prior to the scheduled termination of the run. As the temperature decreased, the drag of the viscous melt eventually broke the seed off the seed holder. The boule then fell into the melt. Fortunately, except for some cracks near the bottom of the boule the entire boule was intact.

The crystal was 140 mm long in the straight section with a diameter of approximately 25 mm. One striking feature of this boule is its highly polished surface as grown. It is believed that this effect is due to both the higher purity feed used and the elimination of leaks in the furnace. Improvements of the surface texture have been observed at MIT for both of these changes. Virtually the entire boule was fabricated into laser rods; interferograms of the rods are shown in figure 16.

Boule 109 Y c

10% Er^{3+}:$LiYF_4$

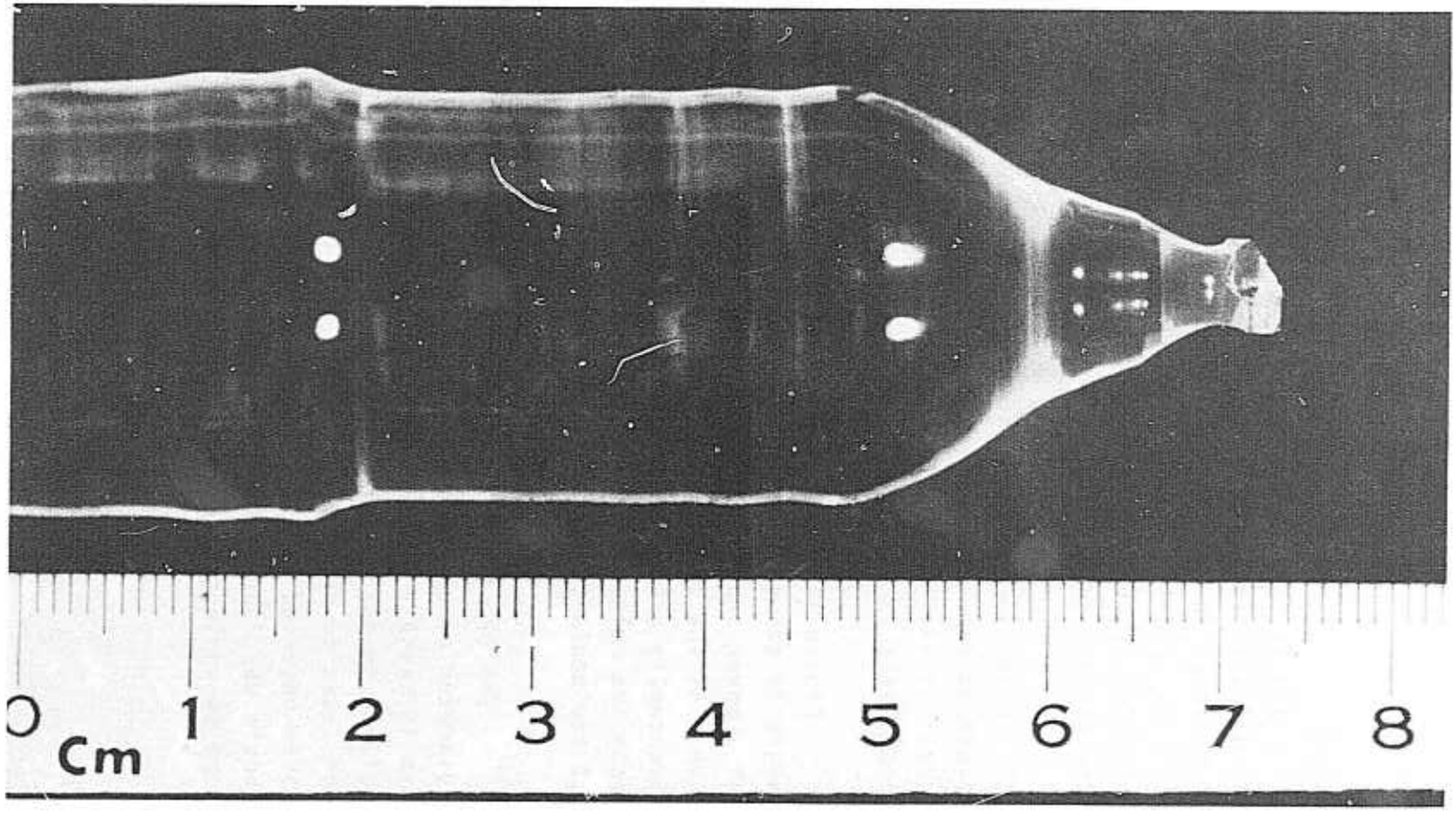

Figure 14. Neck of boule 109 Yc.

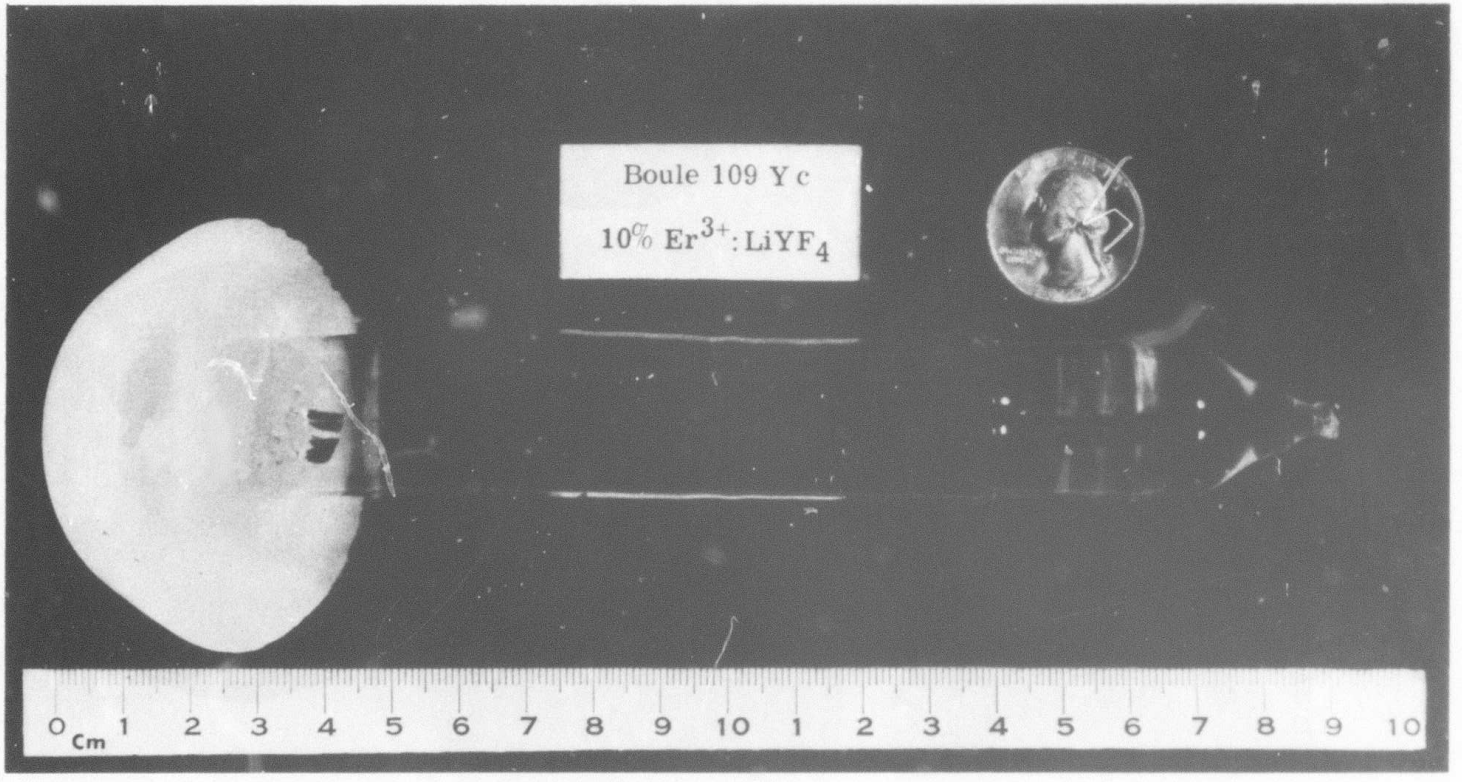

Figure 15. Boule 109 Yc.

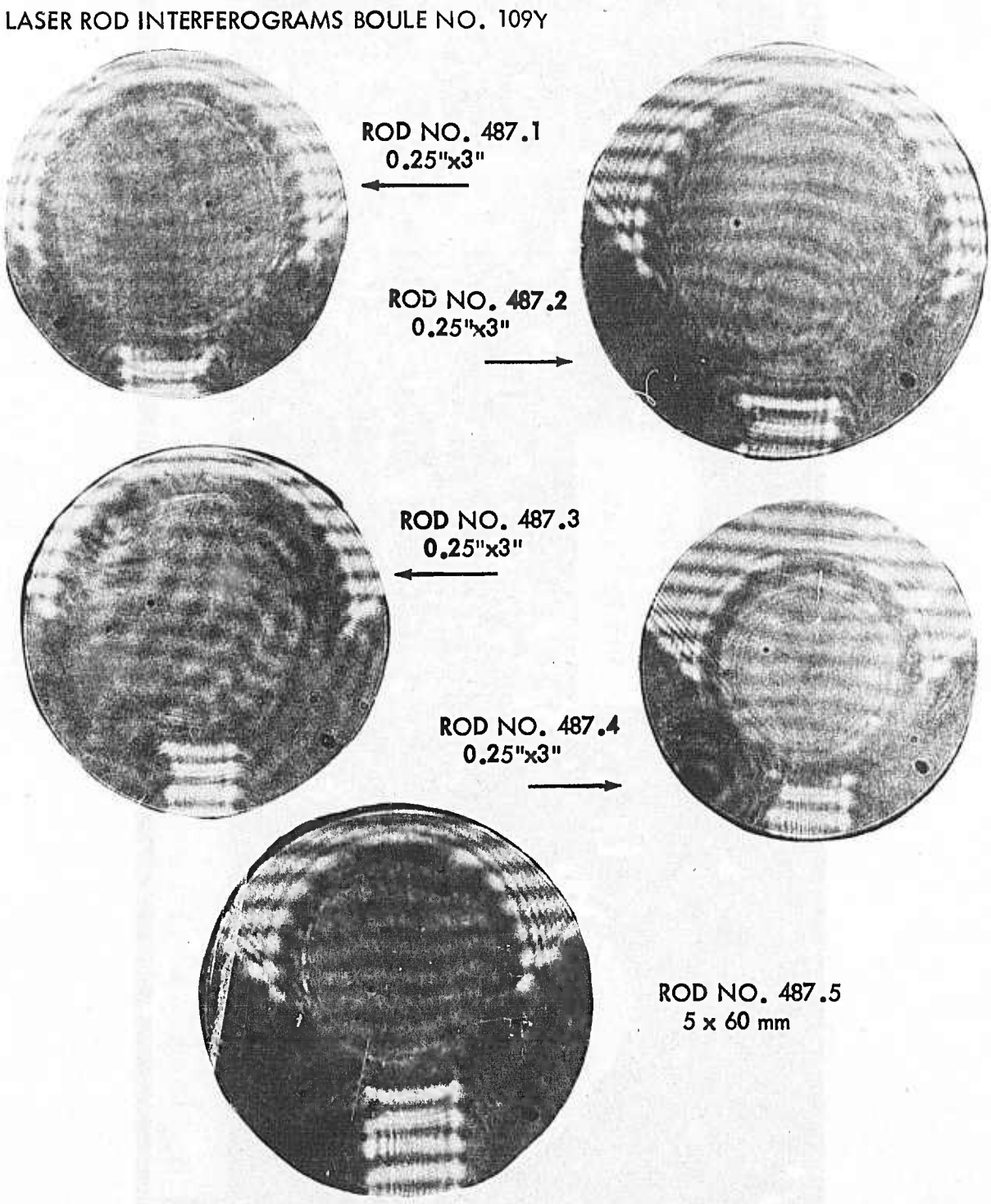

Figure 16. Boule No. 109 Y Interferograms.

2.3 CRYSTAL GROWTH PARAMETERS

Based upon the investigation of a number of crystal growth parameters, improvements have been made in the growth process. It is generally accepted that the growing interface should be flat to slightly convex into the melt to promote uniform mass transfer and strain free growth. In setting up the furnace at Sanders Associates, adjustments to the thermal shielding were made which increased the gradient in the growing crystal, and thereby influenced the interface to take on the desired form.

The rate at which the growing boule is rotated has also been reduced from a high of around 60 rpm to 25 rpm. This has resulted in an increased smoothness of the as grown crystal wall and a desirable melt/crystal interface form.

Experiments at MIT/CPL have confirmed the effect of rate upon interface shape under gradient conditions and rotation rate associated with the furnaces there. To study the interface shape Er:YLF cryatals were seeded and grown in the usual way. After several cm of growth, the crystal was rapidly disconnected from the melt. Figure 17 shows a longitudinal section through the solid-melt interface (the cut surface was blackened to demark the interface shape) of a YLF:Er boule grown at 40 rpm. This concave shape is one that was commonly observed in many crystal growth runs. Figure 18 shows the interface shape obtained at a rotation rate of 15 rpm. This is decidedly convex and in much more desirable form. It should be noted that rotation rate and thermal gradient work in concert to influence the interface shape and the optimum rate may diff . from furnace to furnace. We find then that in the Sanders Associates crystal growth system a rotation rate of 25 rpm is appropriate for while in the MIT/CPL system 15 rpm appears to be more satisfactory.

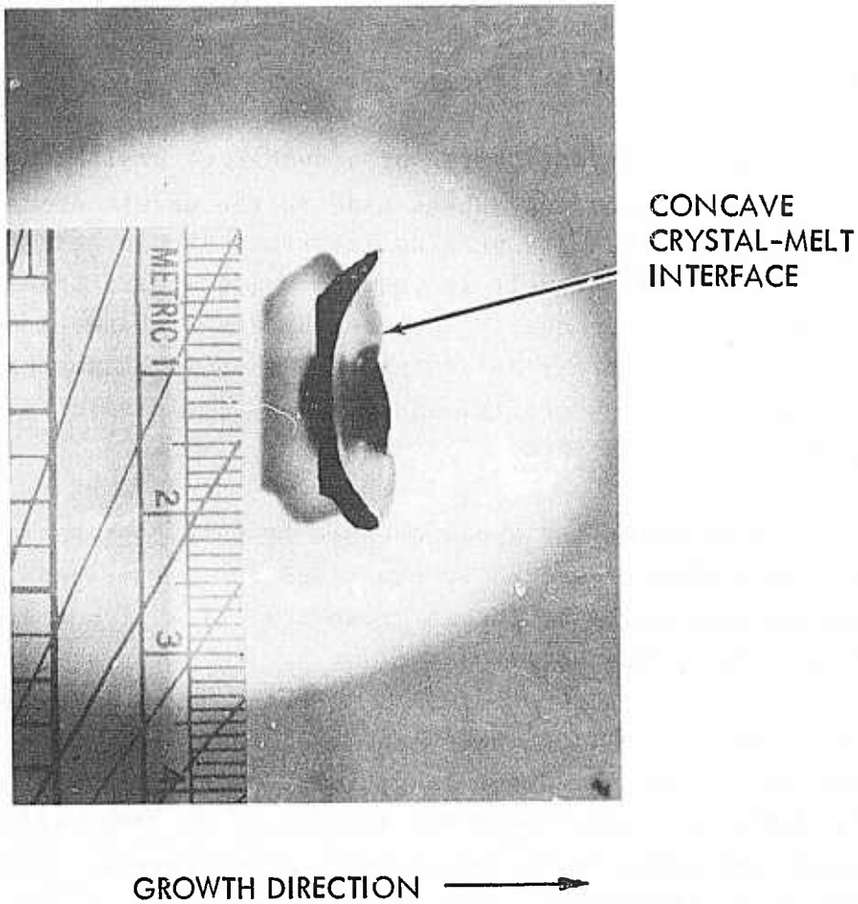

Figure 17. Slice of $LiYF_4$ showing the effect of growth at 40 rpm.

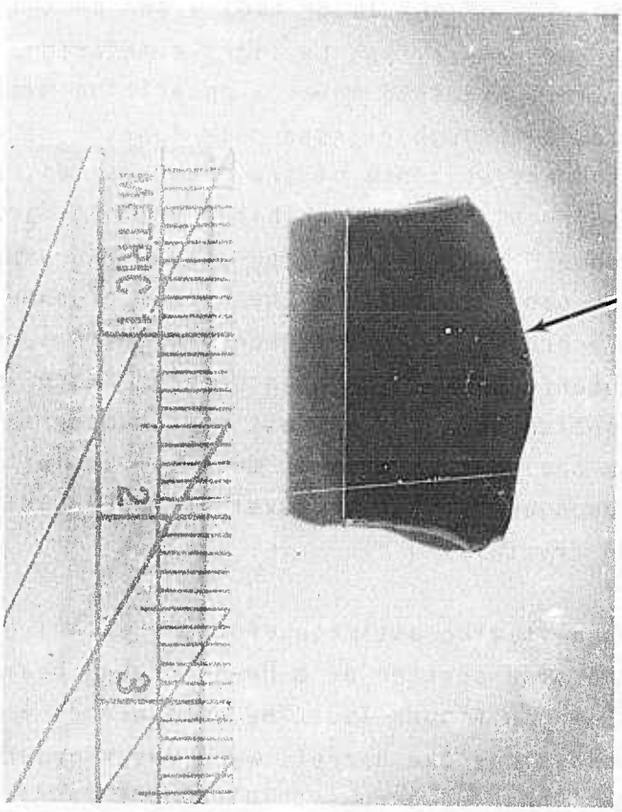

Figure 18. Slice of $LiYF_4$ showing the effect of growth at 15 rpm.

2.4 LIGHT SCATTERING MEASUREMENTS

The optical quality of the laser rods grown on this program was assessed by interferometry and by light scattering. In addition, crystals were examined under a polarizing microscope and a polariscope. Viewed through crossed polarizers none of the YLF laser rods exhibited any evidence of grain boundaries, rods viewed along their length in this manner exhibited uniform dark and light fields depending upon orientation of the axes with respect to the polariscope. Small samples cut from the bottom of some of the boules exhibited low angle grain boundaries when viewed in a polarizing microscope. The interferograms shown in section 2 are indicative of the very high optical quality of most of the material grown in this program. For the most part, this material exhibits far superior optical homogeneity (lower level of index variations) than YAG or other oxide crystals.

To obtain a qualitative estimate of the scattering in the laser rods, photos of the side scatter of a He-Ne probe beam were recorded. The results are shown in figure 19. The entire rods were immersed in an index matching fluid since the barrels were rough ground. The rods are outlined by dashed lines and arrows point to the faces.

The exposure (120 sec at f 11) was chosen so that the scattering in the prints corresponded to that visually observed in a dark room. The contrast of rod 458.1, grown on a previous program, with the other two rods is indicative of the improvement in the optical quality of this material which has been achieved on this program.

Several experiments were attempted in order to obtain a quantitative estimate of light scattering. Measurement of the threshold energy versus coupling mirror reflectivity[4,5] yielded results which were not self-consistent. This may have been due to the use of uncoated rods in the measurement. Because of time constraints, this approach was abandoned.

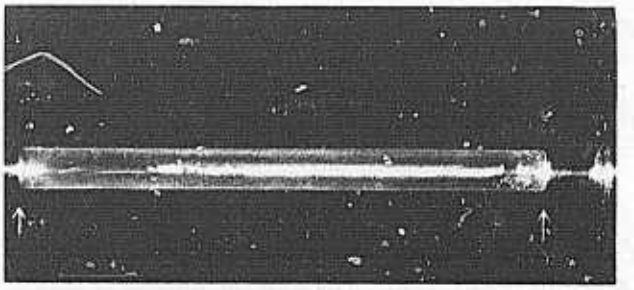

ROD 458.1; BOULE 203F
GROWN: 1974

SOURCE: 1mW He Ne

INDEX MATCH: GLYCERIN, n = 1.473

EXPOSURE: 120 SEC. AT f-11

FILM: ASA 3000

MAGNIFICATION: 1:1

SPEED: f-11

ROD 476.1; BOULE 106YB
GROWN: DEC 1974

ROD 479.5; BOULE 108Y
GROWN: JAN 1975

Figure 19. Light scattering in Er:YLF.

The approach finally adopted was a direct transmission measurement. Unfortunately Er^{3+}:YLF absorbs at .6328 μm eliminating He-Ne as a probe. Attempts were made using Er^{3+}:YLF operated at 20 Hz illuminating samples external to the resonator. The transmitter laser light was monitored with and without the test sample. The long term stability of the laser was remarkably high but the low duty cycle and trigger generated RF made accurate measurement impossible.

Finally, the direct approach shown in figure 20 was adopted with good results. A 150 watt Xe arc lamp was focused into a pinhole then collimated to a beam width of 4 mm. Transmission measurements of an optically thick Er:YLF sample were recorded to assure that absorption in the crystal would not influence the results. Er:YLF exhibits no absorption between 0.849 to 0.940 μm; interference filters centered at 0.855 μm were chosen for the measurement.

Care was taken to assure that the measurements were not influenced by artifacts. In particular, the beam was well collimated and the detector aperture was larger than the beam. In this way the attenuation of the entire beam is measured. With a detector smaller than the beam erroneous results were obtained; in some instances the transmitted light increased when the sample was inserted. This is probably due to the nonuniform beam intensity which is altered somewhat in the presence of the sample.

The results for uncoated and AR coated rods are shown in table 3. The results represent the average of at least 5 measurements. Each measurement was made by removing the sample, adjusting the signal for 100 arbitrary units in the lock-in by tweaking the S-1 PMT voltage, then inserting the sample and recording the transmitted intensity. The rods were inserted at normal incidence to the beam.

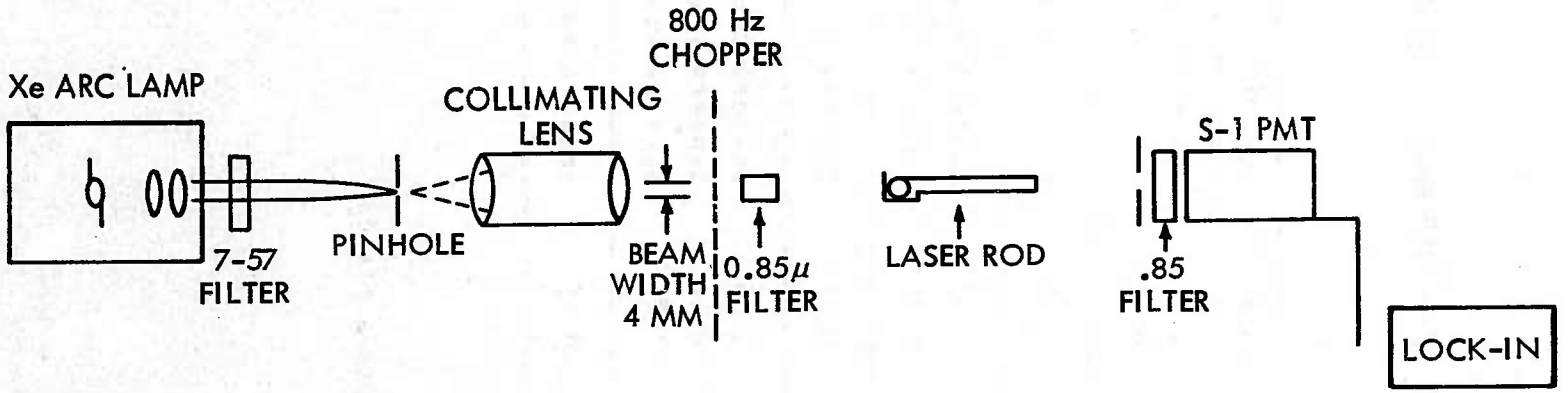

DETECTOR ACTIVE AREA : 0.5 CM^2

PROBE BEAMWIDTH : 4 MM DIA.

A = .12 CM^2

Figure 20. Light scattering measurement.

TABLE 3. SCATTERING COEFFICIENT OF Er:YLF RODS AT 0.855 MICRONS

Rod Number	Length (cm)	T (%)	α(% cm^{-1})	Remarks
446.1a	5.0	87.5	1.2	MIT boule 180f+
463.2	6.0	88	0.94	
472.2	6.7	88	0.84	MIT boule 220f
487.1	7.62	90.5	0.37	Sanders boule 109 Y
487.5	6.1	90.5	0.46	Sanders boule 109 Y
476.1	7.62	88.5	0.67	Sanders boule 106 Yb
487.2*	7.62	97	0.35	Sanders boule 109 Y
487.3*	7.62	98	0.21	Sanders boule 109 Y
487.4*	7.62	98	0.21	Sanders boule 109 Y
479.3*	7.62	97	0.35	Sanders boule 108 Y

* AR Coated with (assumed) 0.2%R per surface

\+ Grown in a He atmosphere

For the case of the uncoated rods the reflection coefficients of the faces were calculated from

$$R_e = \left[\frac{n_e-1}{n_e+1}\right]^2 \text{ and } R_o = \left[\frac{n_o-1}{n_o+1}\right]^2$$

for the extra ordinary and ordinary rays, respectively, at normal incidence. At .855 μm

$$n_e = 1.4719 \text{ and } n_o = 1.4495;$$

so

$$R_e = 0.036$$
$$R_o = 0.034.$$

Because the beam was unpolarized, we take the geometric mean

$$R = \sqrt{R_o R_e} = 0.035.$$

This is necessary because all the samples used were "a" axis rods.

Now the transmission of a plane parallel plate taking into account multiple reflection is given by

$$T = \frac{(1-R)^2 e^{(-\alpha x)}}{1 - R^2 e^{(-\alpha x)}}$$

where α is the scattering coefficient (the absorption at this wavelength is too small to measure), x is the path length, and T is the measured transmission. Because R is small we can neglect the denominator (i.e., neglect multiple scattering). We obtain

$$\alpha = \frac{1}{x} \ln \frac{(1-R)^2}{T}.$$

The results, tabulated in table 3, also include measurements on AR coated rods where a reflectivity of 0.2% per surface (the vendors specification) is used.

The estimated reading error is ±0.5 divisions; for rod 487.1 this translates to

$$\alpha = 0.37 \pm 0.07 \quad \% - cm^{-1}$$

Systematic errors are more difficult to quantify. Residual absorption in the wings of the filters is probably not significant as the rods with the lowest scattering loss will have the highest absorption (487.1 - 10% Er). Viewing the unfiltered beam in a darkened room showed scattering only from the faces of the rods (all the rods were cleaned prior to the measurements but some of the rods were scratched). Lastly, the acceptance angle of the detector was small but finite; and some forward scattering might be included in the measurement of T. This depends to some extent on the degree of collimation of the probe beam. Changing the acceptance angle by a factor of two did not significantly affect T; so forward scattering does not seem significant. It is interesting to note that the AR coated rods exhibit a uniformly lower α than the uncoated rods. This may be due to the fact that the surface finish on the coated rods was generally higher.

The results of this measurement together with the interferograms shown in figures 9, 13 and 16 show that the growth technique has produced rods of uniformly high optical quality.

2.5 REMARKS

The object of this part of the program was to investigate the means of obtaining and to produce Er:YLF of very high quality. To some extent, these goals are conflicting and in this program "production" took precedence over "investigation." As a result, it was not possible to systematically investigate all conceivable variables of the growth and feed purification techniques. Nevertheless, we have demonstrated that:

a. Growth of YLF in an argon atmosphere has resulted in reproducibly high optical quality material (low index variation and low scattering).

b. Automatic diameter control improves the reproducibility, perfection, and yield of laser material.

c. Boule size is currently limited by geometry of the current crucible and associated furnace components.

d. Rods with scattering less than 0.5% cm^{-1} and path distortion much less than 1 fringe per inch have been grown with good reproducibility.

3.0 FEED PREPARATION

3.1 GENERAL

In this section the different techniques used for preparation and purification of the feed for the growth will be described. These involve methods applicable to commercial fluorides as well as to fluorides produced by wet chemical prepurification. The success of these techniques is clearly evidenced by the optical quality and very low light scattering level of the crystals grown. However, they are by no means definitive due to the supposition of various minor furnace and processing problems upon the growth experiments and to temporal constraints.

Two separate and successful lines of feed preparation have been followed, one employing commercial fluoride feed directly, the other involving wet chemical prepurification and synthesis of a fluoride feed using the commercial oxide for the process input. These two paths are shown in Figure 21.

3.2 HYDROFLUORINATION OF MOLTEN $LiREF_4$

In the former method, developed originally at Sanders, and used for all but one of the growth runs, anhydrous YF_3 obtained from Research Chemicals and LiF (Harshaw chips) in the desired proportions are melted together in flowing HF at 900°C for about five hours in an Inconel reactor. The charge is contained in a vitreous carbon boat. After such treatment the $LiYF_4$ is generally fairly well crystallized. The material is then physically pre-cleaned before it is loaded into the furnace. A similarly treated batch of $LiErF_4$ is prepared for use as dopant material.

As was indicated in a previous report[3] using this technique completely scatter-free YLF was grown.

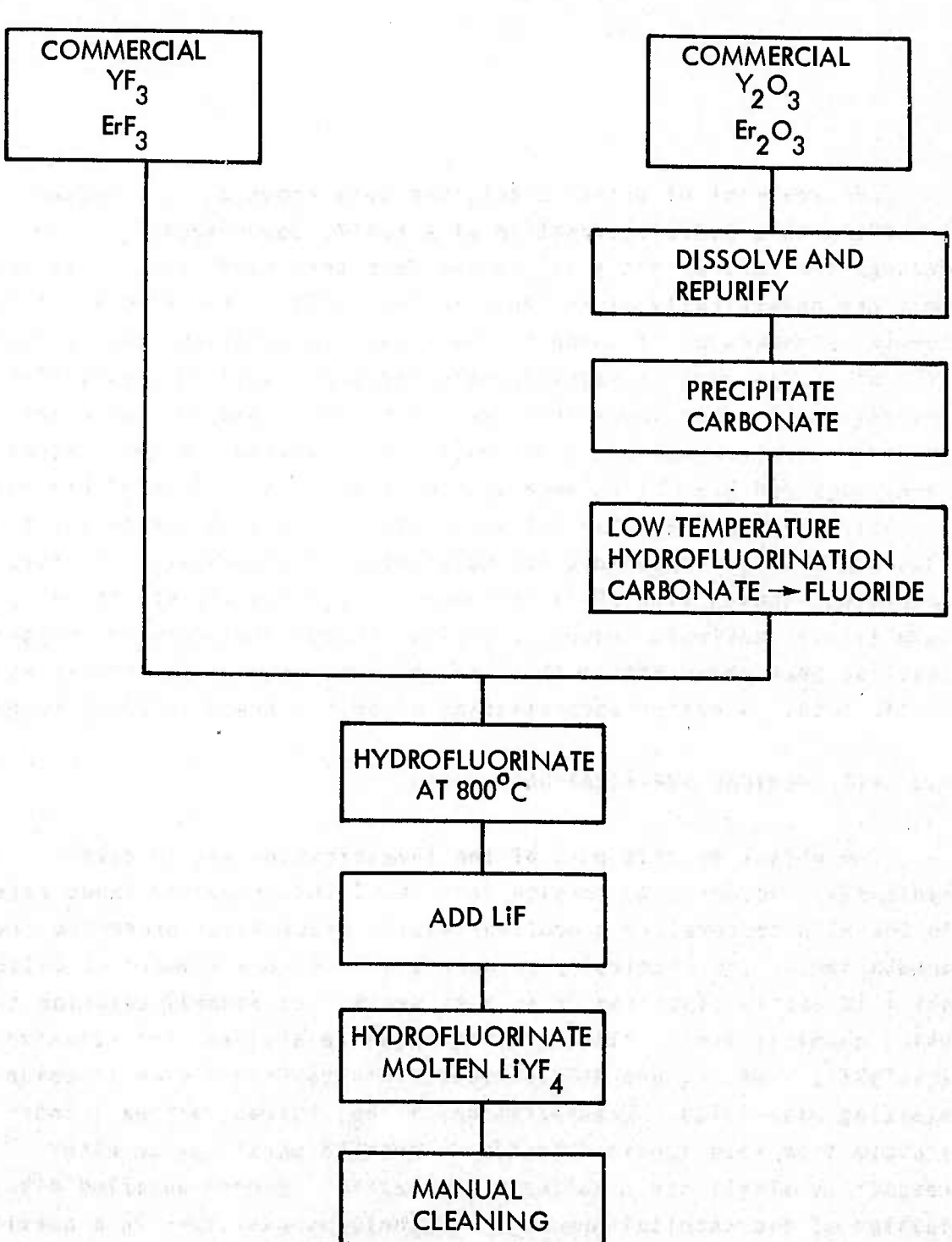

Figure 21. Feed preparation flow chart.

HF treatment of molten $LiREF_4$ has been shown to be a better procedure than hydrofluorination of a solid, powdered REF_3. The reasons for this probably lie in the fact that diffusivities in the melt are dramatically higher than in the solid. This allows for more complete conversion of oxide to fluoride. In addition, the surface area of the product is significantly reduced, avoiding substantial absorption of water vapor from the atmosphere. Thus we can expect a lower level of oxygen and other volatile impurities in the pretreated $LiYF_4$ compared with $LiYF_4$ made by comelting in Ar untreated LiF with YF_3 prehydrofluorinated in the solid state. This is not to say that oxygen alone is responsible for scattering in fluorides. The more complete reaction with HF is believed to have had the effect of solubilizing cationic trace impurities through the decreased oxygen level so that, even though they are present, they do not appear as a precipitate. A better understanding of this process is being sought.

3.3 WET CHEMICAL PURIFICATION

The object of this part of the investigation was to develop synthesis procedures to provide consistent, high quality input material to the high temperature hydrofluorination process for producing crystal growth feed. The chemical procedure starts with a commercial oxide which is easily dissolved in acid to provide an aqueous solution to which chemical purification processes can be applied (the relative insolubility of YF_3 and REF_3 obviates this technique with fluoride starting materials). Precipitation of the desired carbonate intermediate from solution is intended to provide purification with respect to alkali and alkaline earth metals. A more detailed discussion of the chemical processing techniques was given in a previous report.[6]

About 350g of $Y_2(CO_3)_3$ prepared from 999.99% Research Chemicals Y_2O_3 and 100 g of $Er_2(CO_3)_3$ prepared from Research chemicals 99.999% Er_2O_3 were synthesized at MIT/CPL by the purification and homogenous precipitation process described in the previous report.[6] The

carbonates were furnished to Sanders for conversion to fluoride by the low temperature hydrofluorination process. A Teflon lined reactor is used to convert to fluoride by the reaction:

$$RE_2(CO_3)_3 + 6HF \rightarrow 2REF_3 + 3H_2O + 3CO_2$$

Inconel flanges were used to close the reactor; these were corroded by the large amount of wet HF generated by the reaction. As a result, the purified feed was contaminated with a small amount of greenish material shown by chemical tests to contain Ni. Further, in the crystal growth run 109Y using this feed, a metallic appearing scum was removed from the melt surface. The x-ray fluorescence analysis spectrum of this material shows that Fe and Ni are the principal components (See figure 22). This corrosion problem was an isolated event which does not occur during high temperature hydrofluorination where the moisture evolved is very small. To avoid the reoccurrance of corrosion the Teflon lined reactor has been equipped with Teflon enclosures.

Despite the above mentioned problem, this feed was successfully used for growth of boule 109Y. This demonstrates that wet chemical purification methods have been developed which are capable of using rare earth or Yttrium oxides of variable purity and converting them to uniform high purity fluorides.

3.4 THE YIELD OF THE CRYSTAL GROWTH PROCESS

The yield of $LiYF_4$ obtainable from a given $LiF\text{-}YF_3$ melt is defined as to the ratio of the maximum number of mols $LiYF_4$ that can be crystallized to the total $LiYF_4$ content of the melt. This ratio is a function of the initial LiF content of the melt and of the compositions of the solid phase crystallized and of the eutectic toward which the liquid composition moves. A plot of this function is shown in Figure 23. At an initial melt composition of 52 mol % LiF the calculated yield is 97%. The actual yield is mechanically limited to about 85-

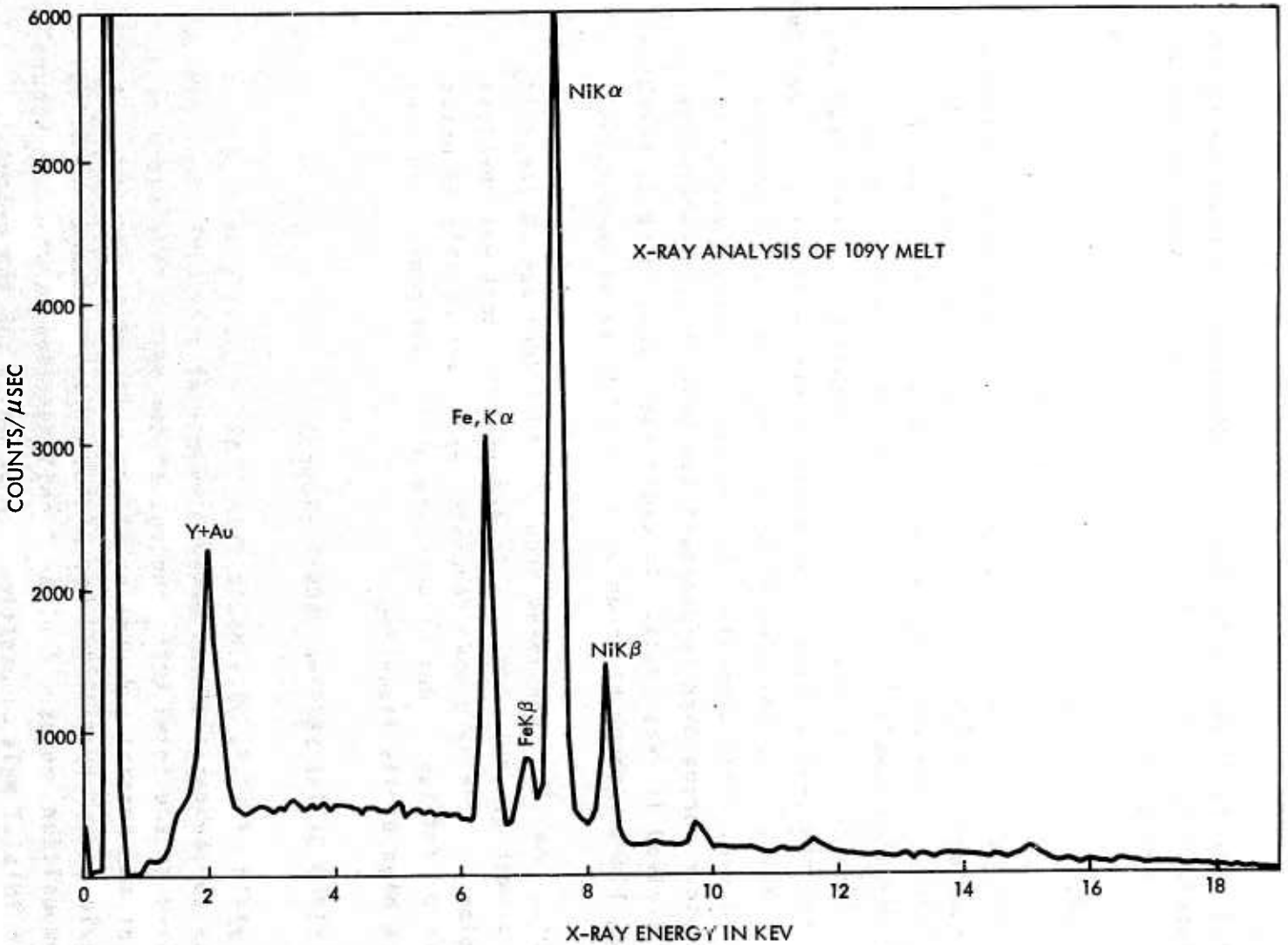

Figure 22. X-ray Analysis of 109Y Scum

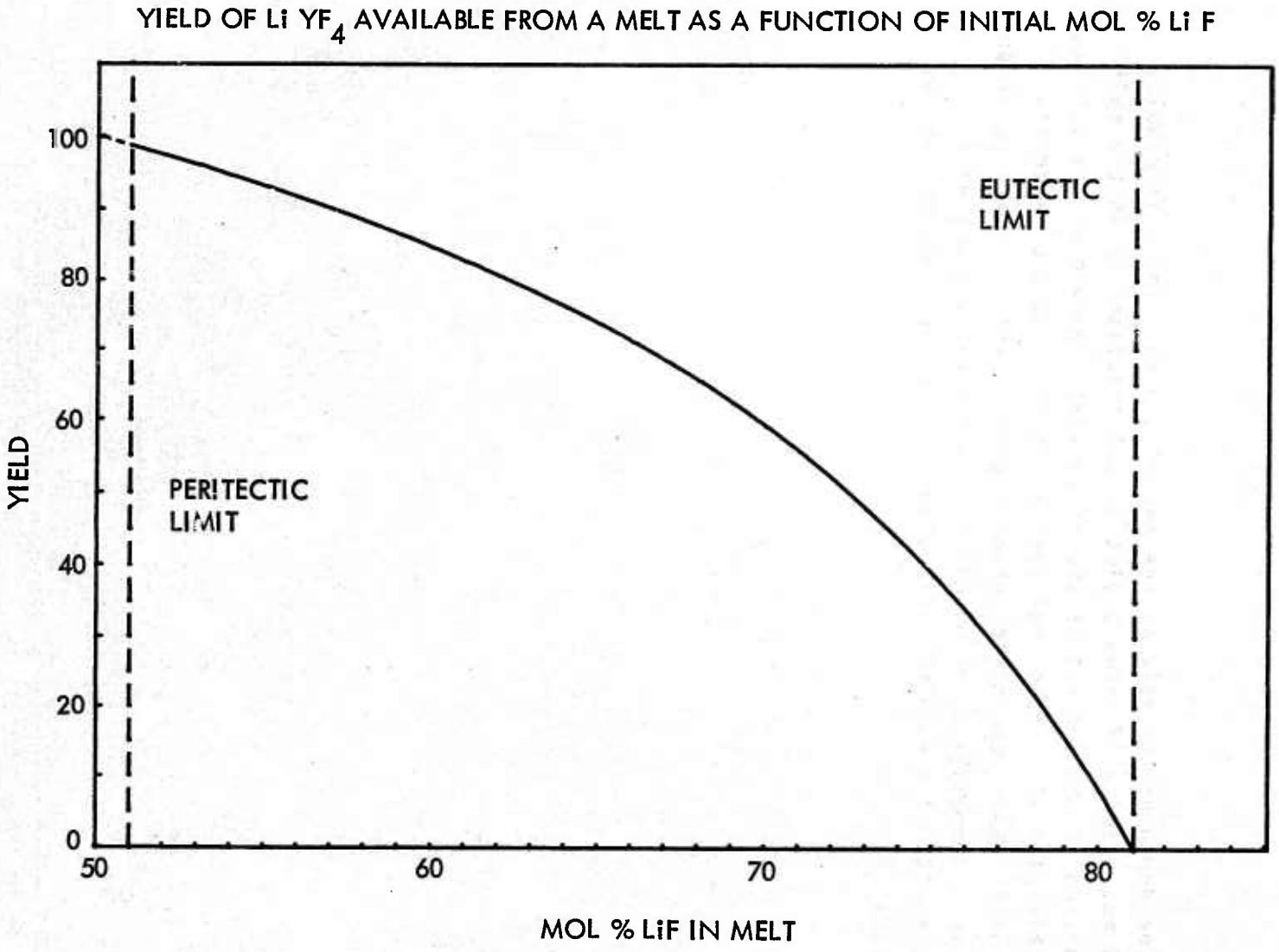

Figure 23. Yeild of $LiYF_9$ as a Function of Initial Mol %LiF

90% by the depth of the melt at the end of the run, which is usually around 5 mm. Figure 24 shows a plot of mol fraction LiF in the melt as a function of the percent of the total $LiYF_4$ removed by crystallization. This plot also shows that over the greater part of a crystal growth run the melt composition changes only slightly. Starting at an initial melt composition of 52 mol % LiF, the LiF content will increase to 64 mol % when 90% of the total $LiYF_4$ has been removed by crystallization.

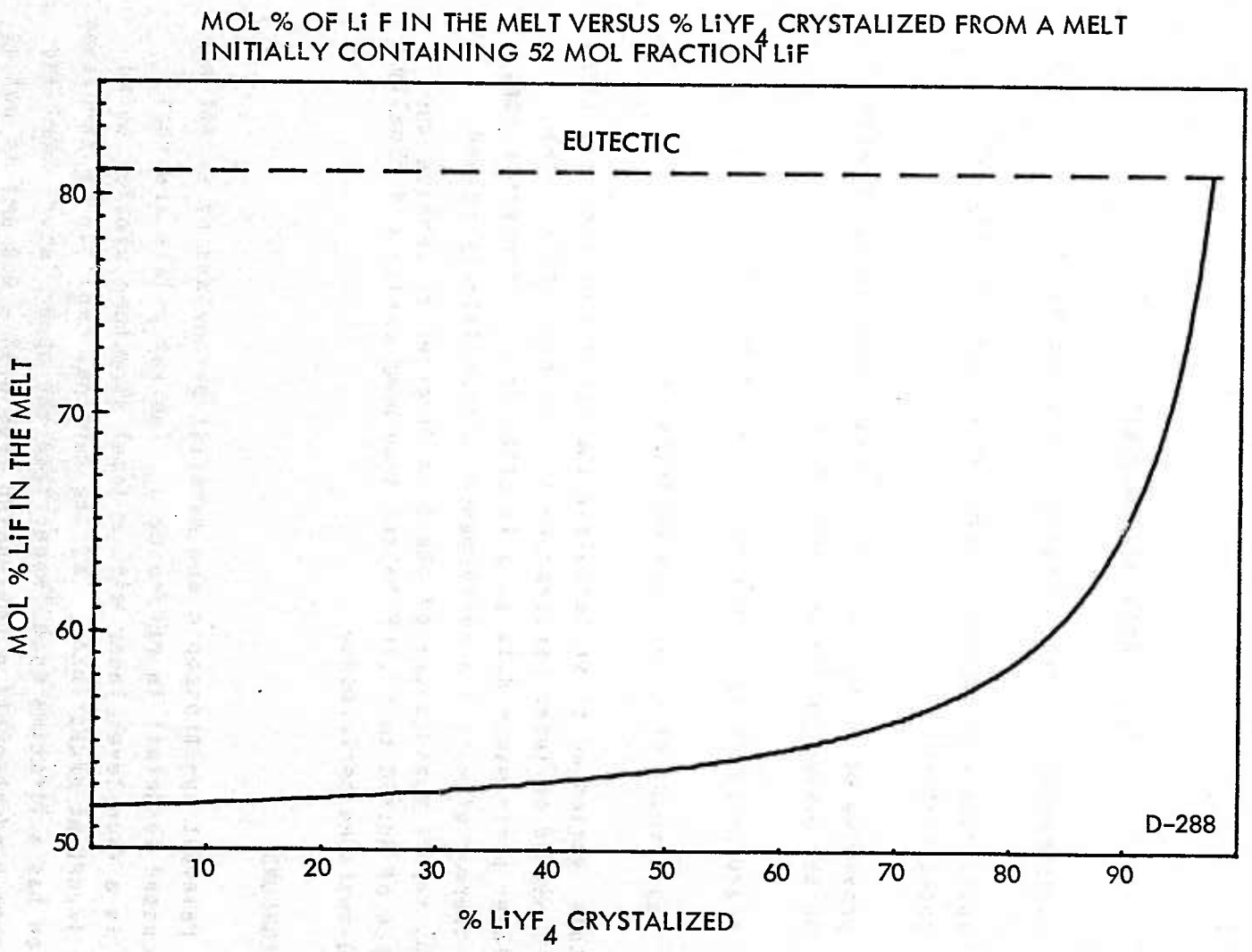

Figure 24. Mol %LiF in the Melt versus %$LiYF_4$ Crystalized

4.0 LASER MEASUREMENTS

Laser measurements in this program were directed at

(a) optimizing the material composition (specifically Er^{3+} concentration)

(b) providing baseline laser performance data at 10 Hz with output powers in the one watt region

(c) measurement of the laser beam divergence and

(d) measurement of Q-switched performance.

In this section we first calculate the effects of the long lived terminal manifold on laser performance at high repetition rates, present laser performance data as a function of Er^{3+} concentration, describe thermal effects and performance in repetitively pulsed operation, report measurement of the beam divergence, compare the performance of Nd:YAG to Er:YLF in the same pump cavity and finally discuss Q-switched performance.

4.1 BACKGROUND

The relevant spectroscopic and material parameters of Er:YLF have been discussed in detail in reference 3. The key points are that Er^{3+}:YLF is a four-level laser with a level structure similar to Nd with two important exceptions: (a) the terminal manifold of the laser transition has a lifetime much longer than the upper laser level and (b) the pump band absorption (extending from 0.55 - 0.2 μm) is not as strong nor as efficiently coupled to Xe flashlamps[3] for the same active ion density. In this section we consider the effect of the long terminal level lifetime on laser performance at high repetition rates, and the effects of Er^{3+} concentration on laser efficiency.

4.1.1 Terminal Level Lifetime

The terminal manifold, $^4I_{13/2}$, of the laser transition in Er^{3+}:YLF is long lived; its lifetime is approximately 13 ms. In reference 7 it was shown that in single shot operation the effect of the long lived terminal manifold was very small, perhaps a 10% reduction of the stored energy which could otherwise be extracted. This is simply due to the fact that the terminal level of the laser transition has an occupation factor of about 10%; if the terminal manifold were a singlet (occupation factor of unity) it is easy to show[7] that only 50% of the initial excess inversion could be extracted.

The case of repetitively pulsed operation bears closer scrutiny. When the interpulse period becomes the order of the terminal manifold lifetime, the possibility of saturation of the inversion must be considered. Equivalently: there may be a practical upper limit in the repetition rate of Er^{3+}:YLF due to population buildup of the long lived terminal level.

Consider a system, shown below, of three levels in which the laser transition is between levels 3 and 2. We assume all ions pumped to level 3 relax to 2 then to level 1. Furthermore we neglect direct pumping to level 2 and out of level 2, and assume the pump lamp provides some initial excitation, N_0, in level 3 during each pulse. Now for a repetition rate, R, (interpulse period 1/R) N_0 decays between pulses according to

$$\exp\left(-\frac{1}{RT}\right) = \varepsilon.$$

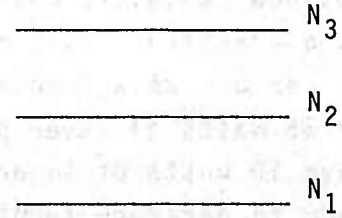

We denote the initial population (after the first pulse) by a.

Just before the second pulse :

$$N_2(n = 1) = \varepsilon a$$

Just before the third pulse:

$$N_2(n = 2) = \varepsilon a + \varepsilon^2 a$$

Just before the n + 1 pulse it is easy to show that:

$$N_2(n = n) = \varepsilon a \left[1 + \varepsilon + \varepsilon^2 + \ldots\ldots \varepsilon^{n-1}\right].$$

We evaluate the asymptotic value of N_2:

$$\bar{N}_2 = N_2(n=\infty)$$

$$= \underset{n\to\infty}{N_2(n)} = \varepsilon a \lim_{n\to\infty} \left[1 + \varepsilon + \ldots + \varepsilon^{n-1}\right],$$

for $\varepsilon < 1$ the series converges to:

$$\frac{1}{1 - \varepsilon}.$$

So the "equilibrium population" of level 2 is simply:

$$\bar{N}_2 = \frac{\varepsilon a}{1 - \varepsilon}, \quad \varepsilon < 1.$$

Let us now calculate whether the terminal manifold lifetime represents a practical limit on the average power attainable in this material. For a 0.25 x 3 inch rod the fracture loading is 83 watts of heat or 56 watts of laser power[3]. At 0.18 times the fracture load we have 10 watts of laser power. We assume an Er^{3+} concentration of 10% (room temperature terminal level lifetime, $T \cong 13$ ms) and we assume 60 Hz operation at 0.167 joules/pulse. Then:

$$\varepsilon = 0.27$$

Now at .85μ there are 4.3×10^{18} photons/joule. In order to obtain 167 mJ/pulse we require 7.2×10^{17} photons; this means that each pulse excites 7.2×10^{17} ions to the terminal level. To account for spontaneous emission from the upper levels, we assume a factor of 2 higher population per pulse ($a = 1.4 \times 10^{18}$). Then the "equilibrium population" is:

$$\frac{\varepsilon}{1 - \varepsilon} (1.4 \times 10^{18}) = 5 \times 10^{17} \text{ ions},$$

or (for a 0.25 x 3 inch rod):

$$\bar{N}_2 = 2 \times 10^{17} \text{ ions/cm}^3.$$

Since the occupation factor of the terminal laser level is about 10% the equilibrium population of the terminal laser level, $\bar{N}_\ell$, is:

$$\bar{N}_\ell = 2 \times 10^{16} \text{ cm}^{-3}.$$

To see if this is significant, this number density must be compared to the threshold inversion. The initial inversion required to get, in this case, 167 mJ per pulse is some initial upper level population density minus the upper level population density, N_T, at threshold. If $\bar{N}_\ell$ is much less than N_T then it will be of no consequence.

With an 85% output mirror and a 3 inch rod the N_T is given by (neglecting scattering losses):

$$N_T = \frac{-\ell n R}{2\ell\sigma} = 7 \times 10^{16} \text{ cm}^{-3}$$

So in this case the initial gain, $N_i - N_T$, is diminished by $\bar{N}_\ell$. This is a small effect but may be observable. For the same average power from a 0.25 x 3 inch rod at the repetition rates shown, $\bar{N}_\ell$ is tabulated in table 4. The last column represents the asymptotic threshold described. It is seen that this effect is significant for repetition rates much above 30 Hz.

TABLE 4

Asymptotic Terminal Level Population vs Repetition Rate at 10 Watts from a 0.25 x 3 inch Rod

Room Temperature

R(Hz)	ε	a (.85 photons/pulse)	$\bar{N}_\ell$ cm^{-3}	$\frac{N_T + N_\ell}{N_T}$
1000	0.92	8.4×10^{16}	4×10^{16}	1.75
100	0.46	8.4×10^{17}	2.9×10^{16}	1.4
60	0.27	1.4×10^{18}	2.1×10^{16}	1.3
30	0.077	2.8×10^{18}	9.7×10^{15}	1.1
10	4.5×10^{-4}	8.4×10^{18}	1.5×10^{14}	1

$\varepsilon \equiv \exp(-1/R\tau)$, $\tau = 13$ ms

a = number of transition from upper to lower manifold (assumed = 2 x photons required for implied energy per pulse)

$\bar{N}_\ell = \frac{\beta}{V} \frac{\varepsilon a}{1 - \varepsilon}$ = asymptotic population in terminal level just before each pulse

β = occupation factor of terminal laser level $\simeq$ 0.1 at room temperature

V = 2.41 cm^3, volume of a 0.25 x 3 inch rod

N_T = threshold inversion for 3 inch rod, 85%R

The assumptions for this calculation are probably pessimistic: most of the upper level fluorescence is to level 1 and we have neglected pumping from level 2 with each flash pulse. Nevertheless, for repetition rates above 30 Hz it might be necessary to add very small amounts of Pr^{3+} to quench the terminal manifold lifetime. For example, with 0.05%Pr^{3+} the terminal manifold lifetime is 3 ms. In this case, for 10 watts out at 100 Hz, ε=0.04, $N_\ell = 1.4 \times 10^{14}$, and

$$\frac{N_T + N_\ell}{N_T} \cong 1.$$

4.1.2 Er^{3+} Concentration

Figures 25 and 26 show transmission spectrum of samples of Er^{3+}:YLF of different optical thickness. Even though the strong peaks are "over absorbed" in the optically thick sample, many weaker bands and the "wings" of the stronger bands do contribute. Figure 26 roughly corresponds to the transmission through a 0.25 inch diameter rod of 10% Er.

It is anticipated from transmission spectra that pumping efficiency should improve with Er^{3+} concentration. In section 4.2, below, laser operation of rods of varying Er^{3+} concentration results in approximately a linear increase of laser efficiency with Er^{3+} concentration from 2-5%Er. The problem with using higher Er concentrations is illustrated in figure 27 where the upper level lifetime is shown as a function of concentration at room temperature. In order to maintain a flash pulse shorter than the fluorescent lifetime (for good efficiency) rather severe lamp loading results. At first it would appear that because the explosion of energy of a lamp can be expressed as the 0.5 power of the pulsewidth,[8] and because the lifetime and laser efficiency versus concentration are measured parameters, then the optimum Er^{3+} concentration for a fixed flashlamp life could be calculated. This is not entirely the case. Flashlamps have a peak current limitation beyond which very rapid degradation occurs due to sputtering of the electrode material. This is discussed in more detail below.

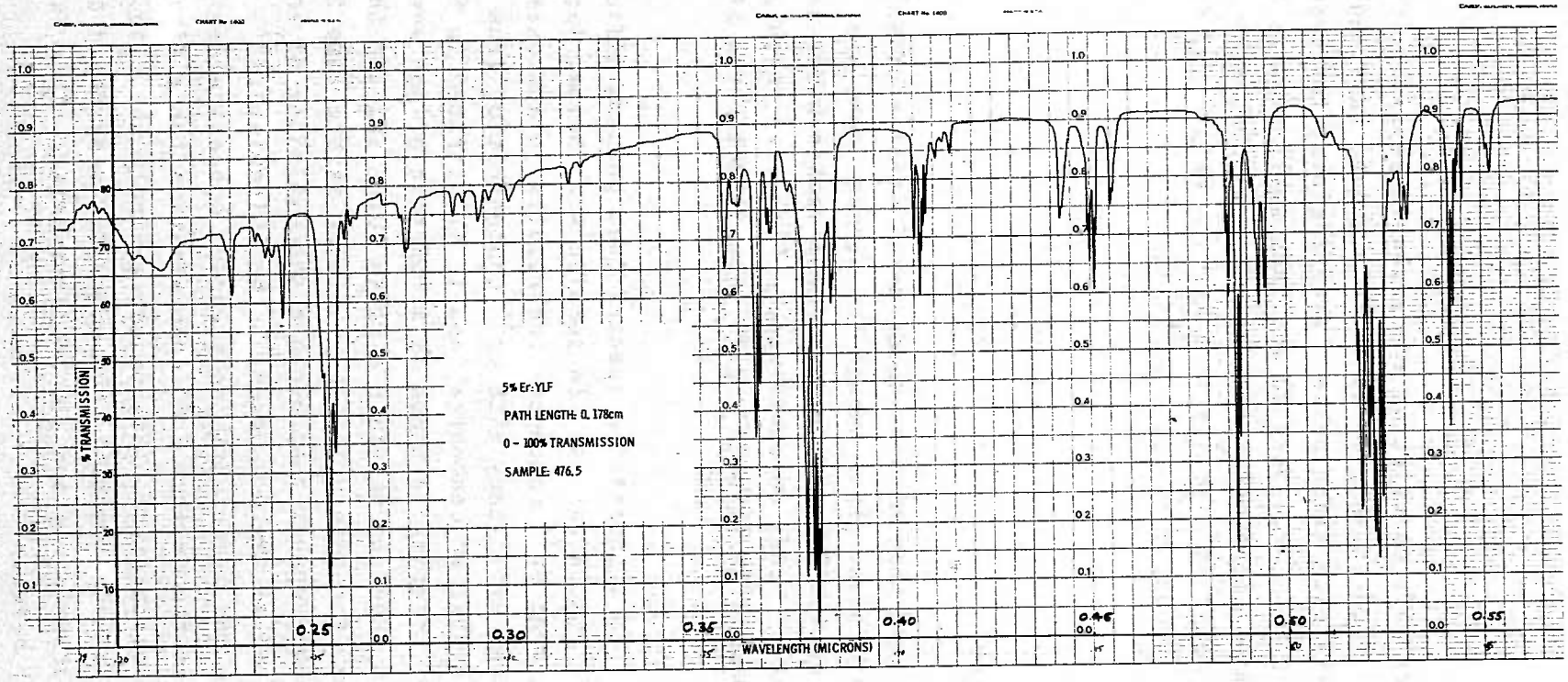

Figure 25. Transmission Spectrum: 5% Er

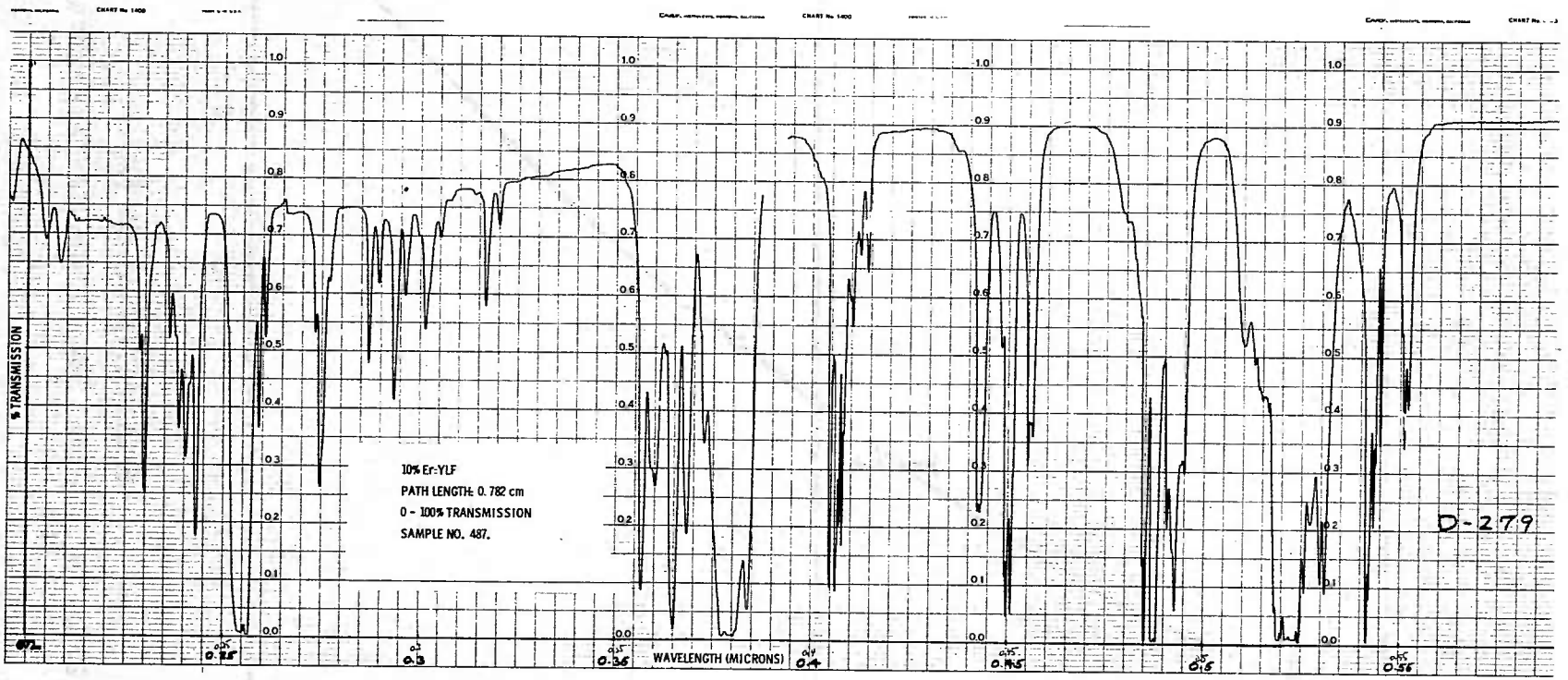

Figure 26. Transmission Spectrum: 10% Er

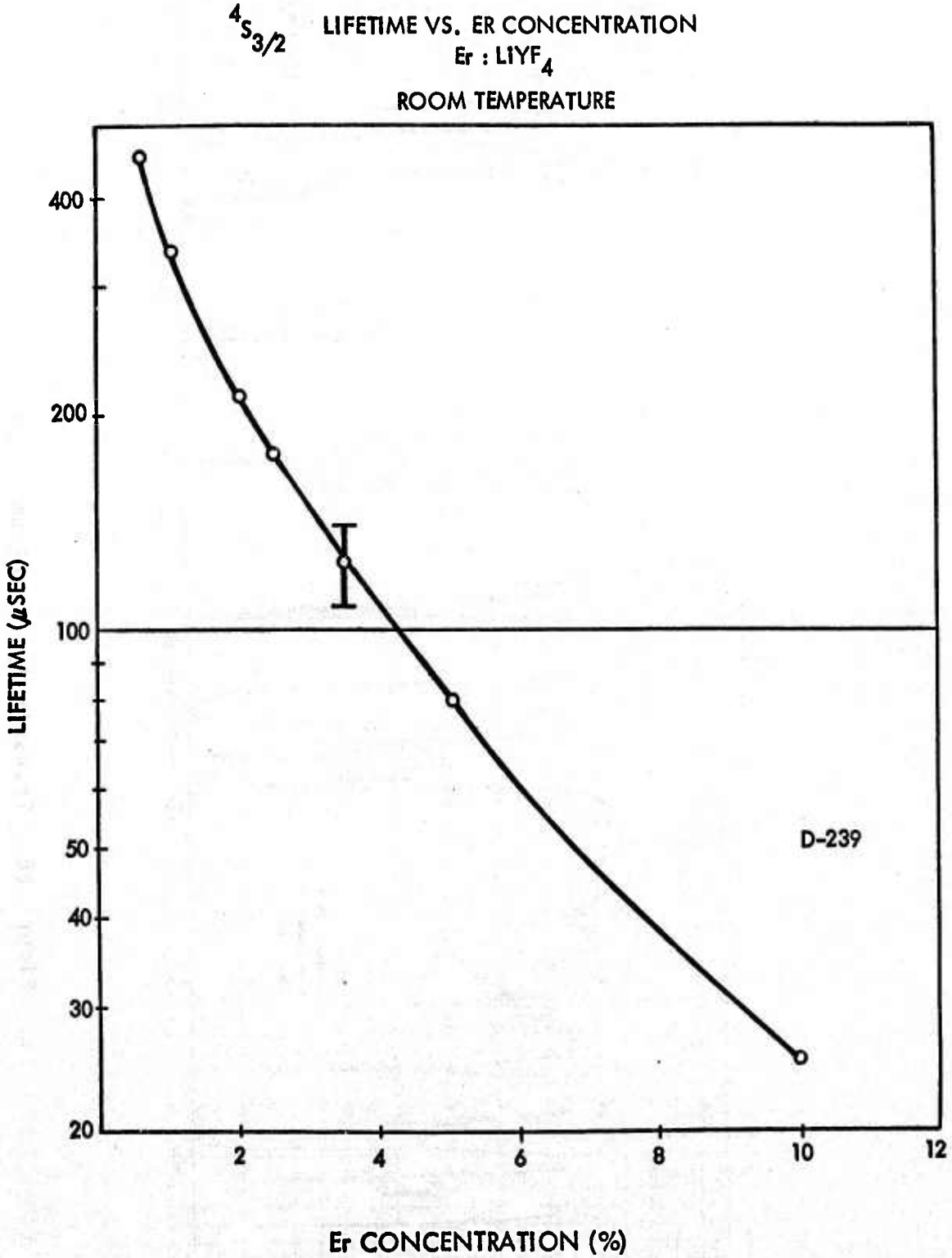

Figure 27. $^4S_{s/2}$ Lifetime Vs. Er Concentration

4.2 LASER EFFICIENCY VERSUS Er CONCENTRATION

A comparison of long pulse single shot and repetitively pulsed operation was carried out in the pump cavity shown in figure 28 using 2% Er, 2.5% Er, 3.5% Er, and 5% Er:YLF rods. The rods were all 5 mm in diameter but the lengths were unavoidably different, ranging from 44-60mm. The pump cavity length, however, was only 36mm so that all other things being equal, shorter rods would be more efficient as the unpumped material simply increases the scattering loss of the resonator. The experimental setup was as follows:

Pump Cavity:	Front surface silver, flooded ellipse (see figure 28) length 36mm
Storage Network:	Single mesh PFN, C = 25μf, L $\tilde{-}$ 0.
Lamp:	ILC 4F-2, 450 Torr Xe
Coolant:	Deionized water at 0.5 - 0.1 GPM.
Flashlamp Pulsewidth:	30-40μs FWHM.
Resonator:	Plane Parallel, 85% R, uncoated rods

Figures 29 and 30 show interferograms of some of the rods used in this comparison. The 2.5 and 3.5% rods in Figure 29 were grown at MIT and show virtually no path distortion.[+] The 5% Er rod, #476.2 shows some path distortion over the 60mm length probably due to the presence of some low angle grain boundaries in the crystal. Scattering in the rods was very low (except for the 2% Er:YLF rod) and could only be observed under He-Ne illumination in a dark room. Scattering inclusions in the 2%Er rod were observable in room light.

Figure 31 shows comparative long pulse data (single shot) taken under very careful conditions in the same pump cavity. The lower energy scale is the input corrected for the lamp/rod mismatch. Only 36mm of the 51mm lamp was in the pump cavity. At the end of the testing

[+]These rods were grown in an argon atmosphere in a previous program (3).

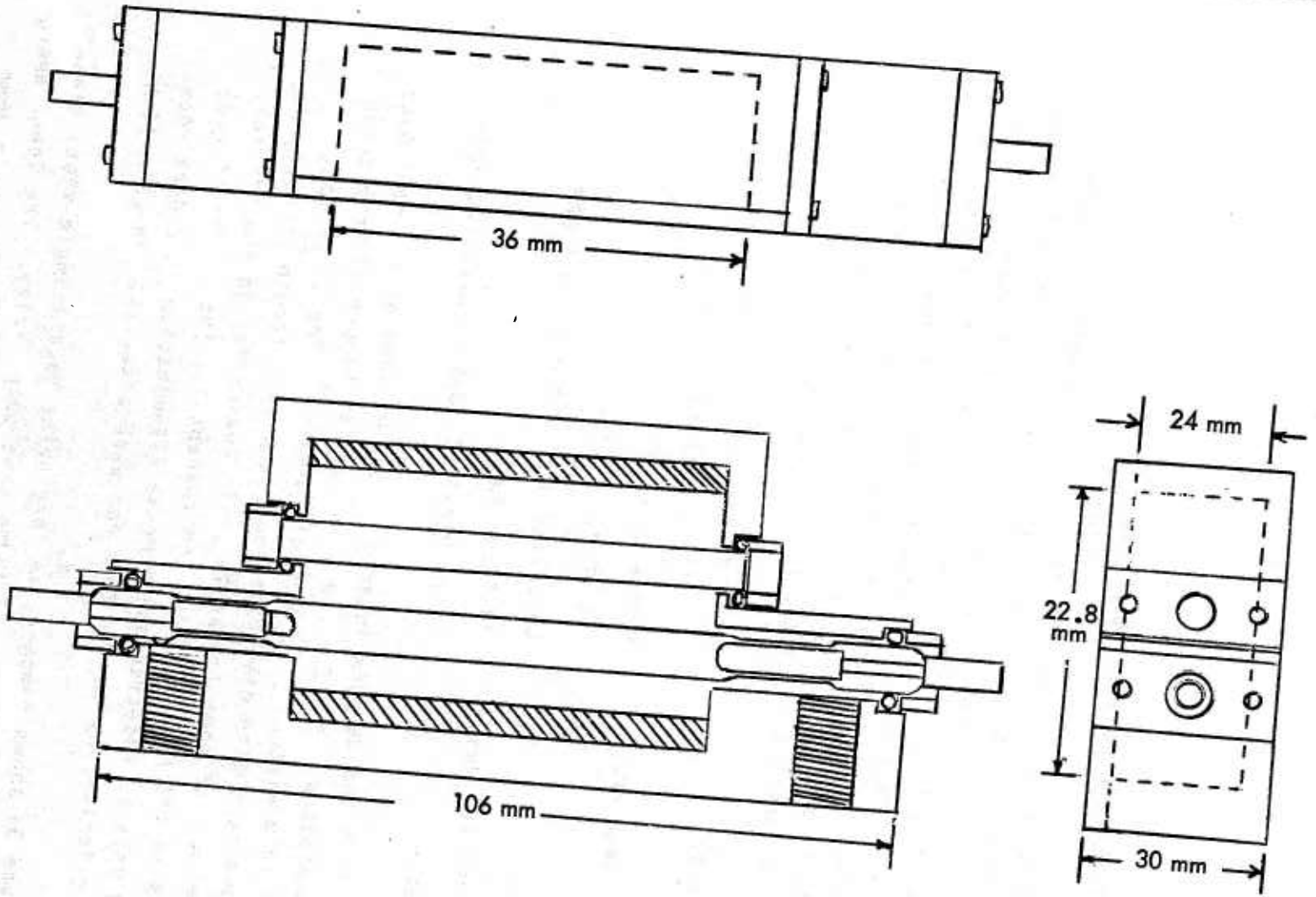

Figure 28. Laser Pump Cavity (5mm rods)

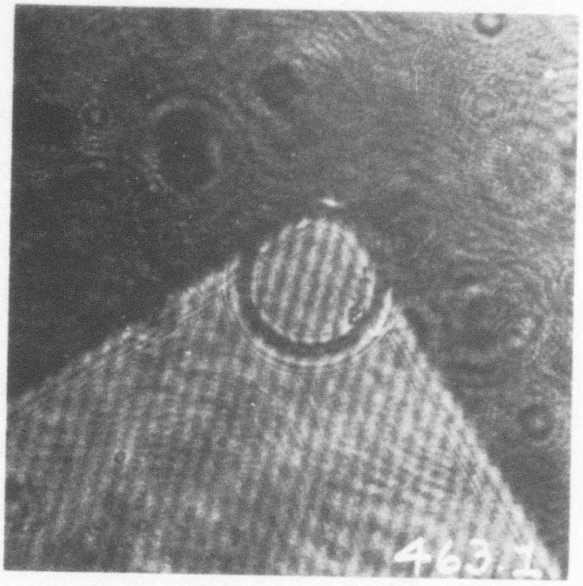

2.5% Er : YLF No. 463.1

5 x 53 mm

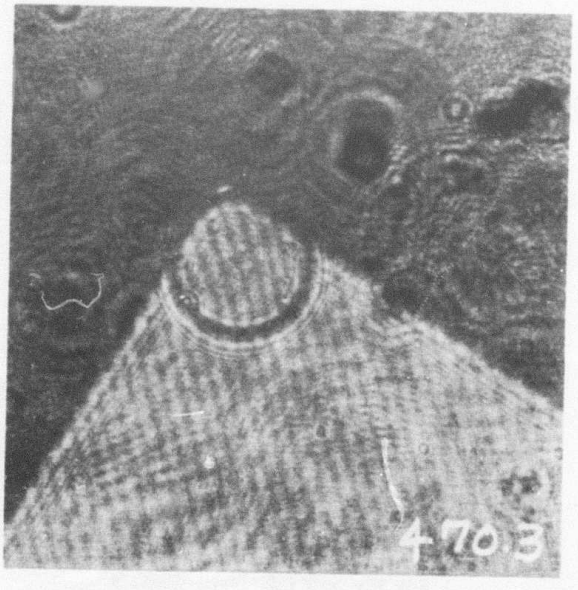

3.5% Er : YLF No. 470.3

5 x 44 mm

Figure 29. Laser Rod Interferograms

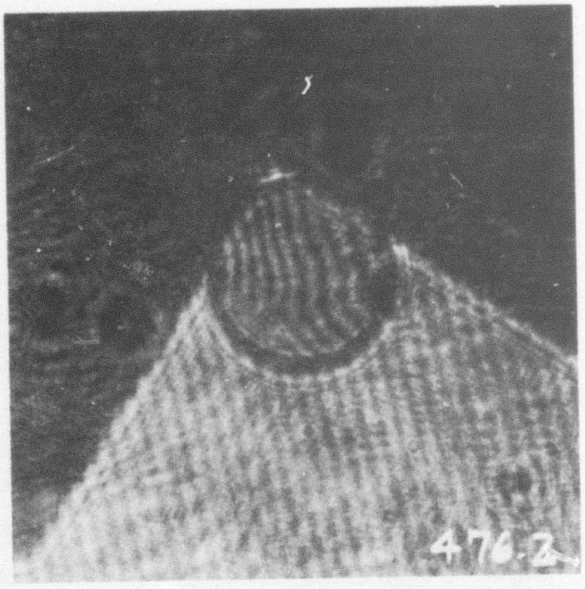

5% Er : YLF No. 476.2
0.25 x 3 INCHES

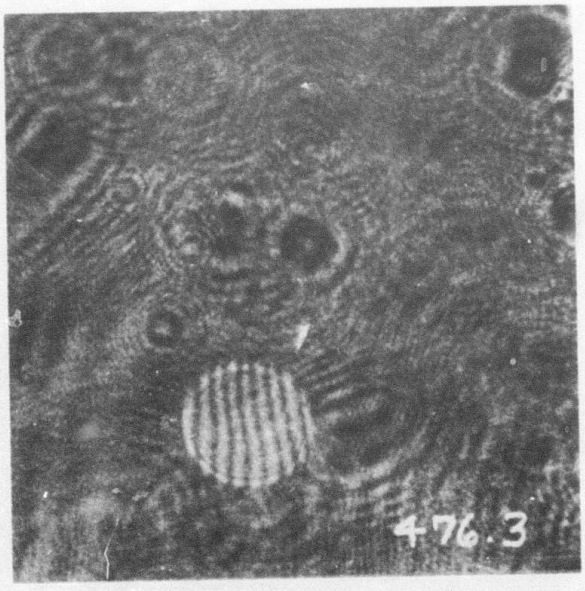

5% Er : YLF No. 476.3
5 x 60 mm

Figure 30. Laser Rod Interferograms

463.1 was remounted in the cavity to assure reproducibility of results. The results were reproducibile to within ±10%.

In Figure 32 the slope efficiency plotted versus Er concentration is seen to be linear in the Er^{3+} concentration. In reference 3 an "optimum" Er^{3+} concentration was estimated based on

(a) the assumption that the pumping rate was linear with the Er concentration.

(b) the measured values of upper laser level lifetime with concentration

and

(c) the assumption of a pump pulse much longer than the upper laser level lifetime.

Solving the rate equations in the steady state we obtained a maximum of the equilibrium population at an Er^{3+} concentraction of 5%; i.e., 5% would be optimum with a pulsewidth longer than the upper level lifetime. In these flashpumped experiments, we have maintained a pulsewidth 30-40μs; the fluorescence lifetimes are 200 and 80μs for the 2 and 5% concentrations, respectively. Under these circumstances, one expects efficiency to scale linearly with concentration as is observed (i.e., assumption (a) is justified). At some point, however, non-uniform pumping effects may become serious. It is anticipated that for 7 mm diameter rods, non-uniform pumping will not be a problem until the Er^{3+} concentration is about 20%.

As the Er concentration increases, however, very serious flashlamp life problems are encountered due to the peak current limitation of the flashlamps and the requirement of maintaining a pulsewidth shorter than the fluorescent lifetime. For example, for the ILC 4F-2 the 500 amp peak current limit is exceeded at about 30 joules with a 40 μs pulsewidth.

OUTPUT VS. ER CONCENTRATION
0.85 MICRONS : ER : YLF

ACTIVE VOLUME 5 x 36 mm
LAMP 450 TORR XE 4 x 51 mm

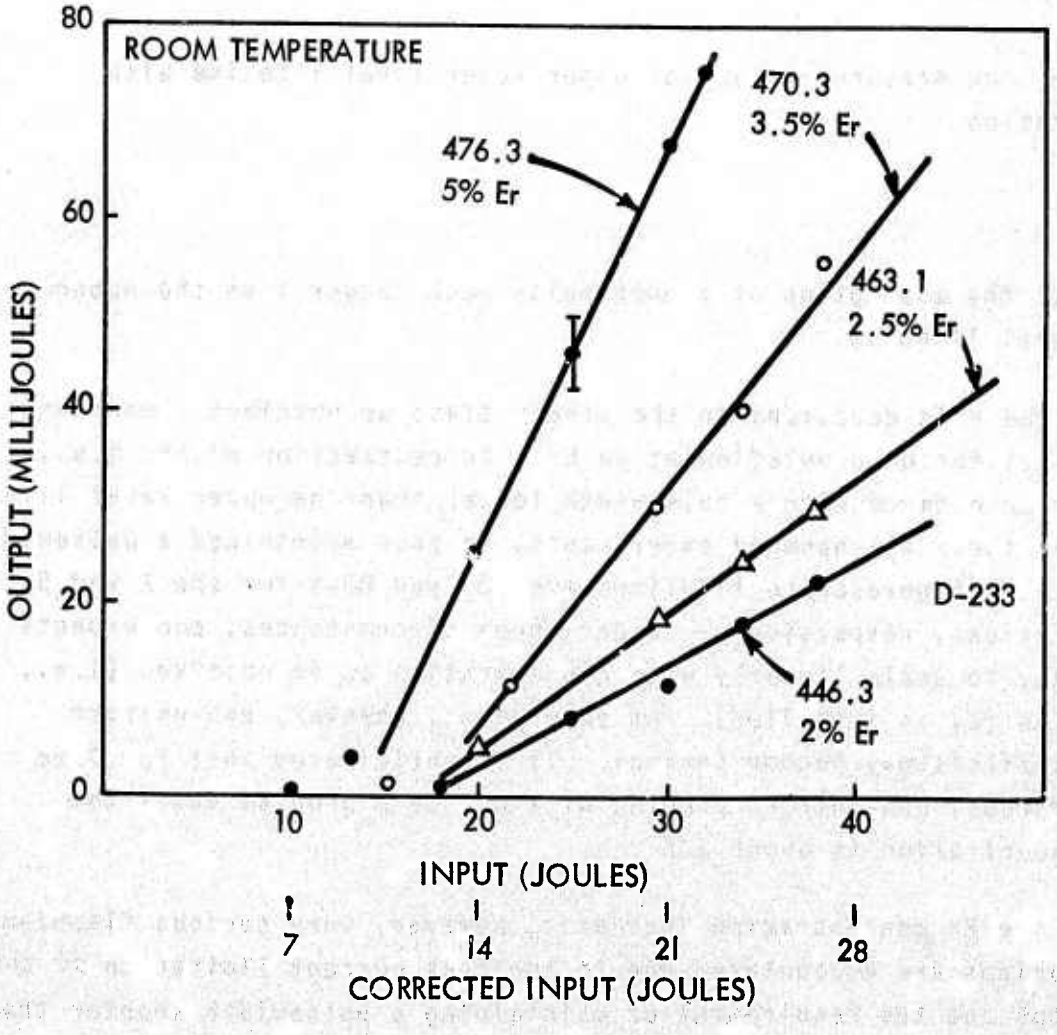

Figure 31. Laser Efficiency Vs. Er Concentration

SLOPE EFFICIENCY VS. ER CONCENTRATION
Er: YLF

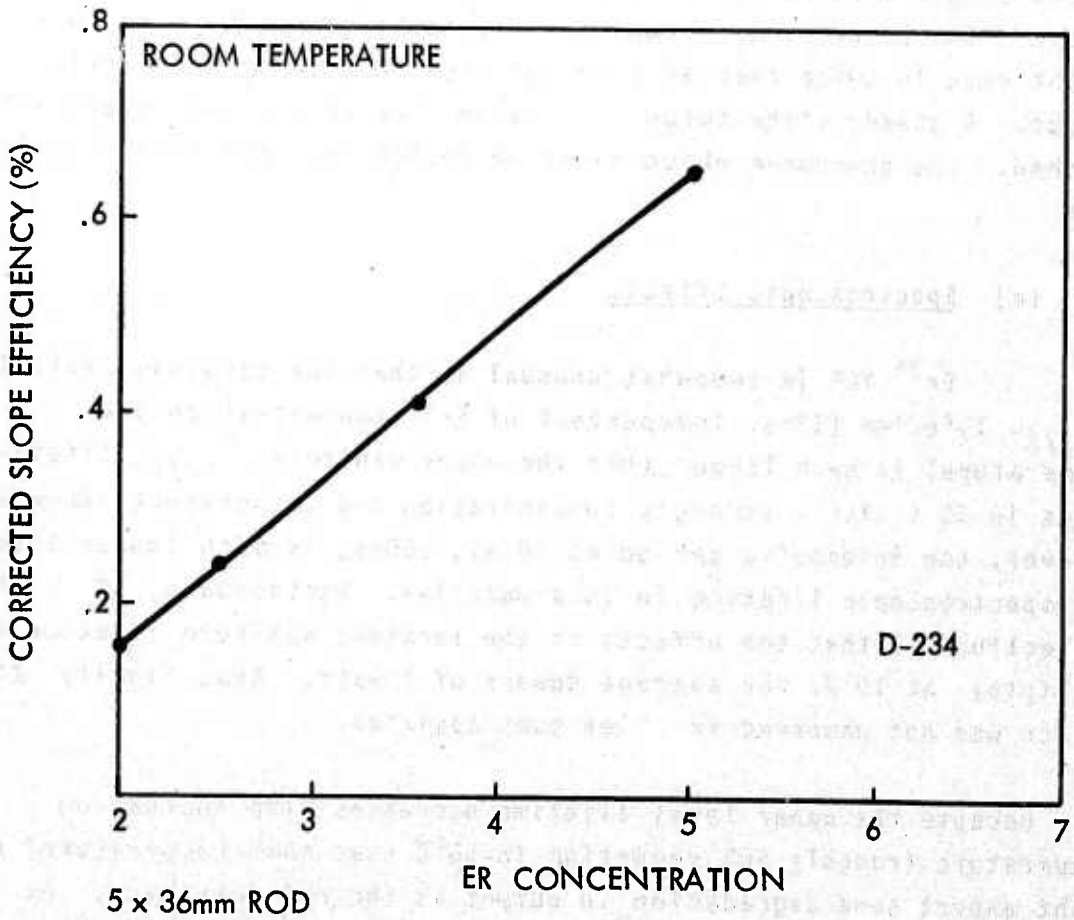

5 x 36mm ROD
4 x 36mm lamp
LONG PULSE - 85%R

Figure 32. Slope efficiency vs. Er concentration.

4.3 THERMAL EFFECTS

Repetitively pulsed measurements were made in the setup described in section 4.2 above. At 5 Hz the measured output power corresponded to the single shot output energy times the repetition rate. At 10 Hz, however, the behavior was complex: in switching from 5 Hz to 10 Hz the output rose to twice that at 5 Hz but then fell below the initial output. A steady state output far below that at 5 Hz was eventually reached. The phenomena which might be responsible for this behavior are:

(a) Spectroscopic Effects

Er^{3+}:YLF is somewhat unusual in that the terminal manifold, $^4I_{13/2}$, lifetime (13ms, independent of Er^{3+} concentration and temperature) is much longer than the upper manifold, $^4S_{3/2}$, lifetime (50μs in 5% Er:YLF - strongly concentration and temperature dependent). However, the interpulse period at 10 Hz, 100ms, is much longer than any spectroscopic lifetime in this material. Furthermore, it is shown in Section 4.1 that the effects of the terminal manifold lifetime are negligible at 10 Hz for average powers of 1 watt. And, finally, this effect was not observed in other pump cavities.

Because the upper level lifetime decreases with increasing temperature (roughly 50% reduction in 50°C near room temperature) one might expect some degradation in output as the rod gets warm. At room temperature the upper level lifetime is about 200μs in 2% Er and 50μs in 5% Er. Because the "quenching" of the output in repetitively pulsed operation in this pump cavity was observed with rods of 2% and 5%, uniform heating of the rod resulting in thermal quenching of the upper laser level lifetime does not explain the data.

(b) Power Supply Effects

Because low values of capacitance are used to maintain a flash-pulse less than the lifetime the power supply must charge to fairly high voltages between pulses. Furthermore, the input energy per pulse goes like the square of the voltage. So a 10% reduction in the charging voltage results in a 20% reduction in input energy per pulse, which can dramatically reduce the output energy per pulse. Careful measurements of the power supply (after several modifications) indicated that inadequate power supply regulation could not account for the observed behavior at these input levels.

(c) Thermal Effects

This seems the only plausible explanation as the characteristic times involved were of the order of hundreds of milliseconds and, more significantly, this behavior was not observed in other pump cavities (cavities where the cooling was more efficient but the optical coupling less efficient). The problem with this interpretation is that the performance characteristics were observed to be roughly independent of average power and very strongly dependent on repetition rate. It was felt that any thermal effect (rise in rod temperature, thermal gradients leading to thermal lensing) would be insensitive to repetition rate changes in the 5-10 Hz region. (i.e., it was assumed that the thermal relaxation time was much longer than 100ms).

The results which are described below indicate that (a) the fall-off above 5Hz is due to a thermally induced resonator misalignment, (b) the thermal relaxation time of the material in this pump cavity is the order of 200 ms, (c) the resonator loss is due to thermal lensing of the rod which can easily be corrected for with a curved mirror, (d) with a 1 meter radius curved mirror the output at 10Hz was double that of 5Hz at fixed energy per pulse.

4.3.1 Experimental

Figure 33 shows recorder traces of the power meter output displaying the power output as a function of time with input energy per pulse and pulse repetition rate as parameters. Stable output at 5 Hz is obtained, more or less independent of the energy per pulse with flat mirrors. At $t = t_o$ the supply is switched to 10 Hz; the output rises immediately, but then falls below the output at 5 Hz. These data were taken with a plane parallel resonator whose alignment was maximized for 5 Hz operation. The optimum alignment at 10 Hz is different; and the steady state output at 10 Hz can be increased after equilibrium. However, it is still far below that at 5 Hz.

In the third trace of Figure 33 the (flat) rear mirror was replaced with a 1 meter radius MAXR reflector at .85. Stable output at 5 and 10 Hz was obtained with the output power proportional to the repetition rate. These results show that a thermally induced resonator misalignment, which could not be corrected for in a plane parallel resonator, accounts for the fall-off at rep rates above 5 Hz. This implies a thermal relaxation time of $\sim$200ms; i.e., at 5 Hz the rod cools down between pulses so the thermal misalignment is not seen even at relatively high average powers. At 10 Hz the temperature of the rod and thermal gradients across the rod increase with increasing average power.

4.3.2 Interferometric Measurements

To check this hypothesis independently dynamic interferometric measurements were carried out using the rod as its own Fabry-Perot interferometer. The reflected beams from the front and rear faces of the rod illuminated by a collimated, spatially filtered He-Ne probe beam were viewed at some distance from the resonator appropriately filtered to eliminate light from the flashlamp.

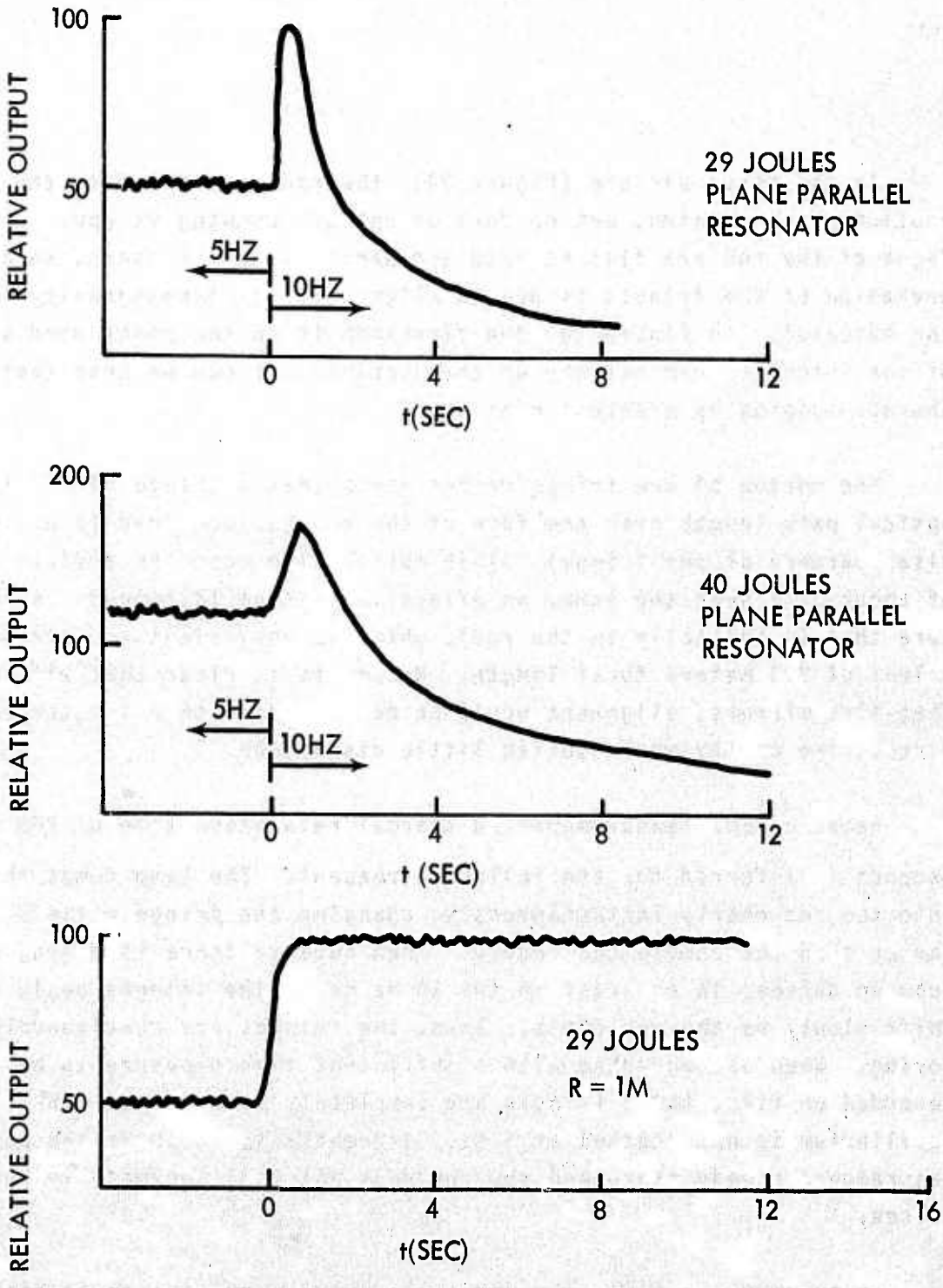

Figure 33. Power Output Vs. Time

In the first picture (Figure 34), the rod is shown with the cooling water running, but no form of optical pumping is applied. The faces of the rod are flat to $\lambda/10$ and parallel to 2 seconds, so any deviation of the fringes is due to slight optical inhomogeneity in the material. In Figure 34, the flashlamp is on the right hand side of the interferogram halfway up the picture. It can be seen that the thermal loading is greatest near the lamp.

The motion of one fringe/fringe means that a change of $\lambda/2$ in optical path length over the face of the rod has occurred (i.e., the disappearance of one fringe). This motion also connotes a distortion of about $3\lambda/2$ near the lamp, an effective tilt of 13 seconds (or much more than is initially in the rod), which is equivalent to introducing a lens of 3.3 meters focal length. Hence, it is clear that with flat-flat mirrors, alignment would be destroyed; with a 1 meter radius mirror, the cavity would suffer little disruption.

Based on 5Hz measurements, a thermal relaxation time of 200×10^{-3} seconds is inferred for the following reasons. The lamp dumps the heat into the rod nearly instantaneously, changing the fringe pattern faster than the camera can record. Then, because there is a long time between pulses, in contrast to the 10 Hz case, the fringes begin to shift slowly as the rod cools. Thus, the fringes are continuously moving. When photographed with a sufficient time exposure to be recorded on film, these fringes are completely washed out. Thus, thermal equilibrium is not reached at 5 Hz. In contrast, at 10 Hz the pattern has reached steady state and the rod does not cool appreciably between pulses.

In summary, at 5 Hz, the rod cools between pulses; so at each pulse, there is no lensing in the rod. The alignment is the same as in single shot operation. At 10 Hz, there is lensing in the rod at each pulse; the alignment is destroyed, and the output power drops.

LASER ROD INTERFEROGRAMS

$P_{IN} = 0$

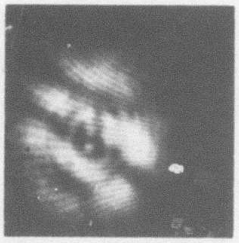

P_{IN} = 40 WATTS
10HZ

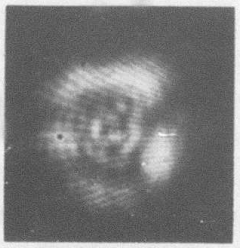

P_{IN} = 200 WATTS
10HZ

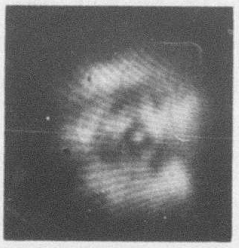

P_{IN} = 300 WATTS
10 HZ

Figure 34. Interferograms of Pumped Laser Rods

4.4 REPETITIVELY PULSED OPERATION

4.4.1 5mm Rods

4.4.1.1 Power Output vs Er Concentration

In figure 35 power output versus power input is plotted at 5 Hz for 476.3 (3.5% Er) and at 5 and 10 Hz 470.3 (5% Er). The same conditions were employed as described in 4.2 above with the following exception. The 10 Hz data (5% rod only) were taken with a 1 meter radius 85%R output mirror. At 300 watts input 0.58 watts output were measured at 10 Hz corrected for the lamp/pump cavity mismatch. The slope efficiency is 0.5% and the overall efficiency is 0.3% at 0.58 watts output.

Using a current probe to measure the peak current into the lamp revealed that at approximately 30 joules input the circuit passed 500 amps. This corresponds to the maximum allowed current for this (ILC4F-2) lamp. Higher input energies (40 - 50 joules) resulted in permanent degradation of the flashlamp efficiency manifest by as much as a factor of two decrease in lasing efficiency. Laser performance could be restored only with a new lamp. This could cause serious experimental problems which could be mitigated somewhat by using longer pulses but at the expense of laser efficiency. In figure 36 comparative performance is shown under identical conditions except for the flash pulsewidth.

4.4.1.2 Beam Divergence

The laser beam width at a distance d = 10.5 meters from the output mirror was measured using a Si photodiode operated in the integrating mode. The laser was operated in the long pulse mode. Care was exercised to avoid diode saturation; the active area was approximately

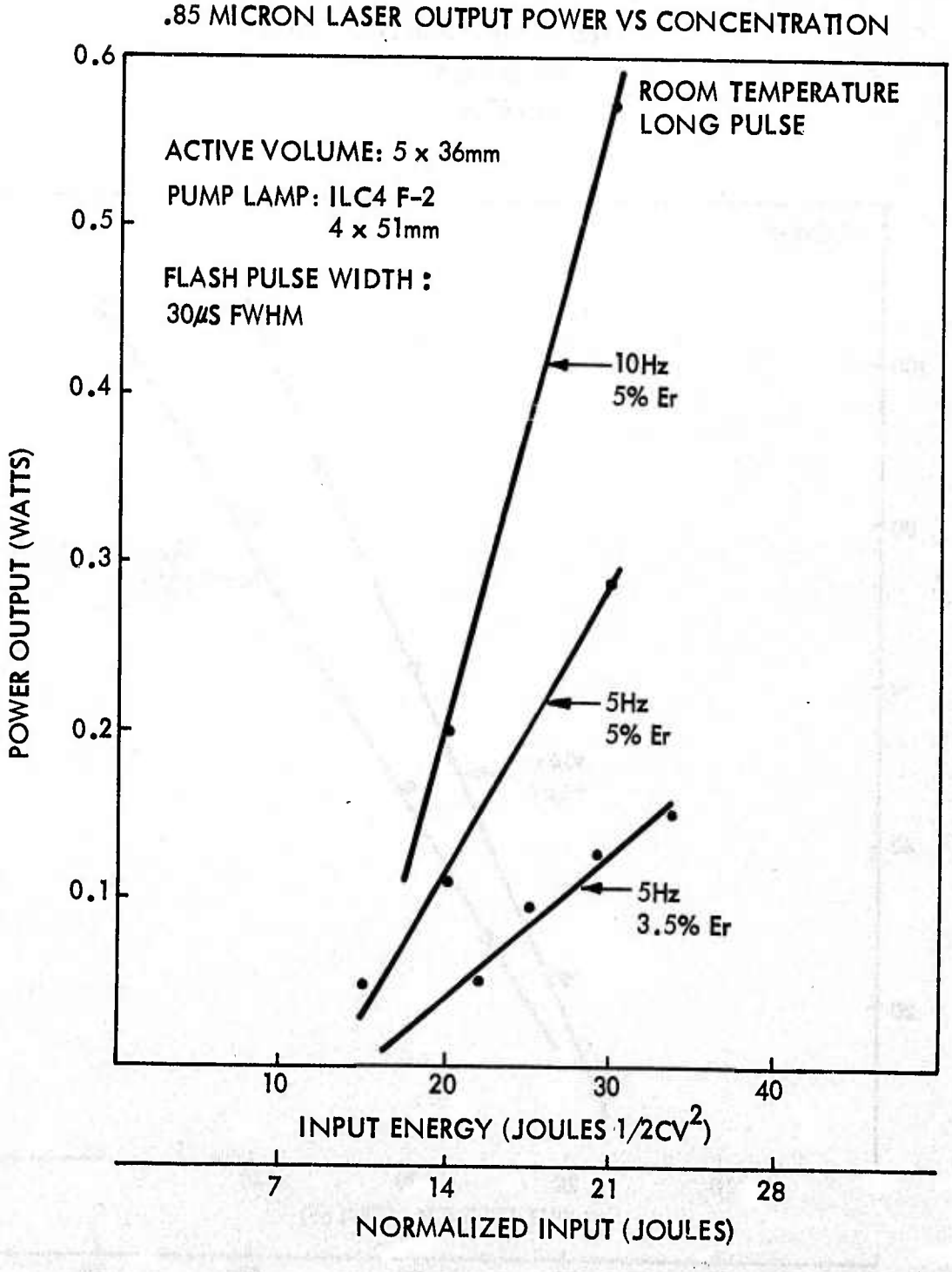

Figure 35. Power Output vs Er Concentration

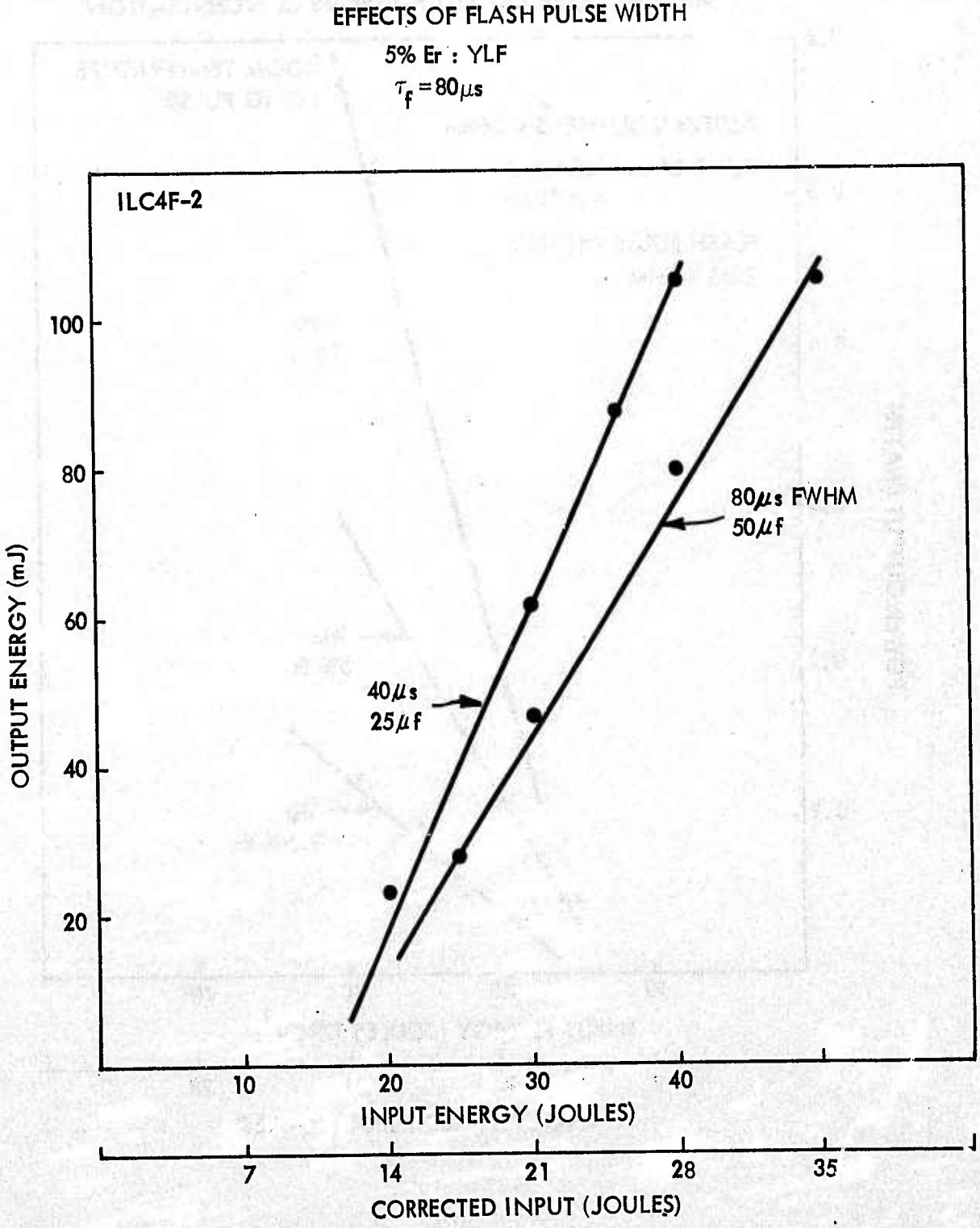

Figure 36. Laser Efficiency vs Flash Pulsewidth

$0.03cm^2$. The results are shown in Figure 37 at 80 watts and 300 watts input to the lamp at 10 Hz. A plane parallel resonator was used with a 5 x 60 mm 5% Er:YLF rod. Only 36 mm of the rod was pumped. At 300 watts input level approximately 0.6 watts output are obtained with a 1 meter radius rear mirror. However, in these measurements only about 50 mW were obtained because of the use of a plane parallel resonator (see 4.3). The resonator lengh was approximately 0.3 meters.

The calculated divergence from these measurements is (full width at the 90% points)

80 watts input: 1.4 mr
300 watts input: 1.5mr

with an estimated accuracy of ±0.2mr. These results were qualitatively checked by viewing the beam reflected off a diffuse surface with an image converter appropriately filtered to prevent blooming. No significant differences in the beam pattern were observed with repetition rate or energy per pulse. These results indicate that the lensing is severe enough to generate resonator alignment problems; but not so severe (at least at these loadings - 150 watts/inch) as to effect degradation of the beam divergence.

4.4.2 0.25 Inch Rods

4.4.2.1 Performance Comparison 7.5% Er:YLF - Nd:YAG

Performance comparison of Er:YLF (7.5%) and Nd:YAG rods were made in a Nd:YAG pump cavity shown in Figure 38. The cavity was converted for use with Er:YLF by recoating the gold pump cavity reflectors with silver. The conditions of the experiment were as follows:

LASER BEAMWIDTH AT 10.5 METERS

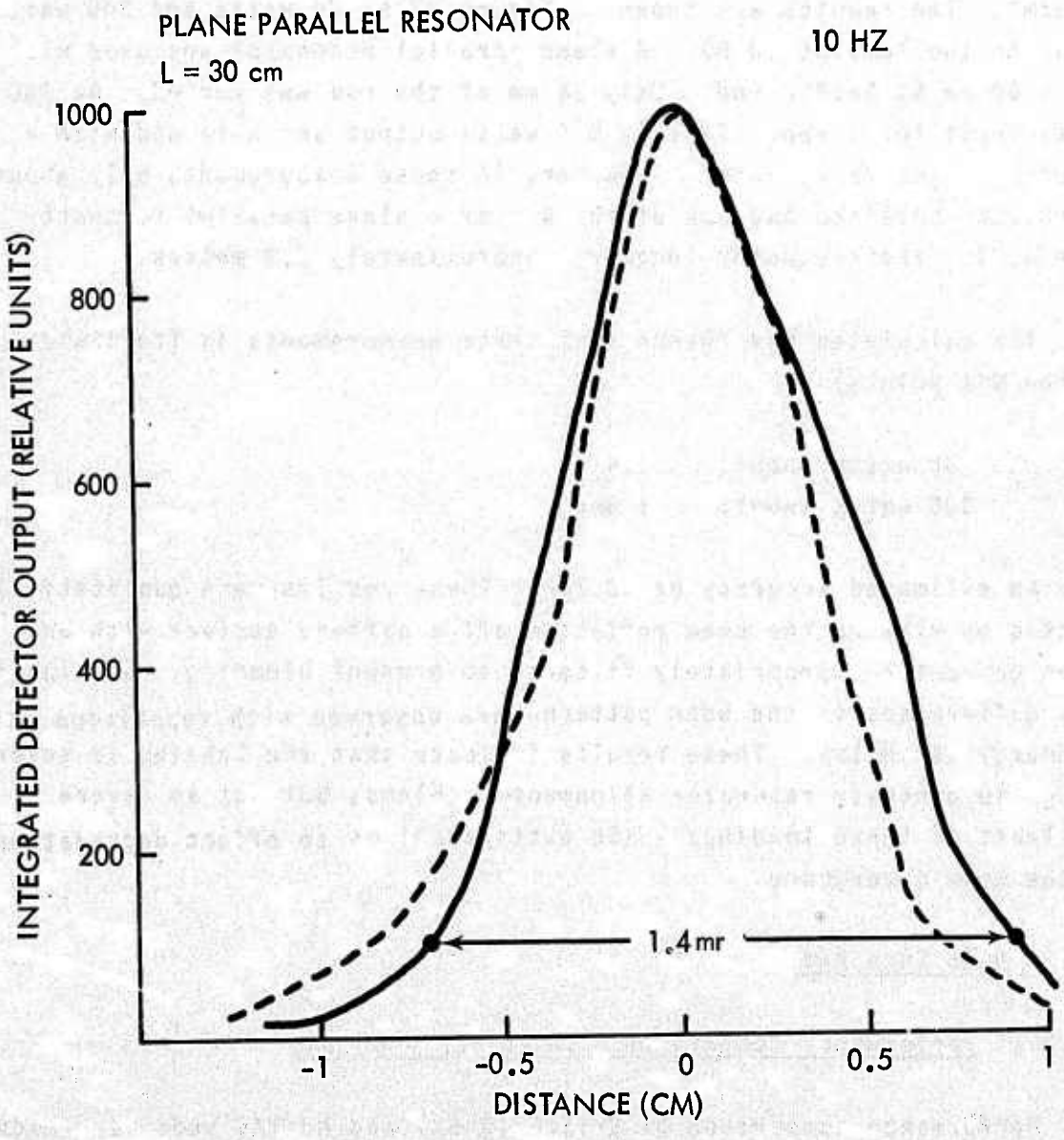

Figure 37. Beam Divergence

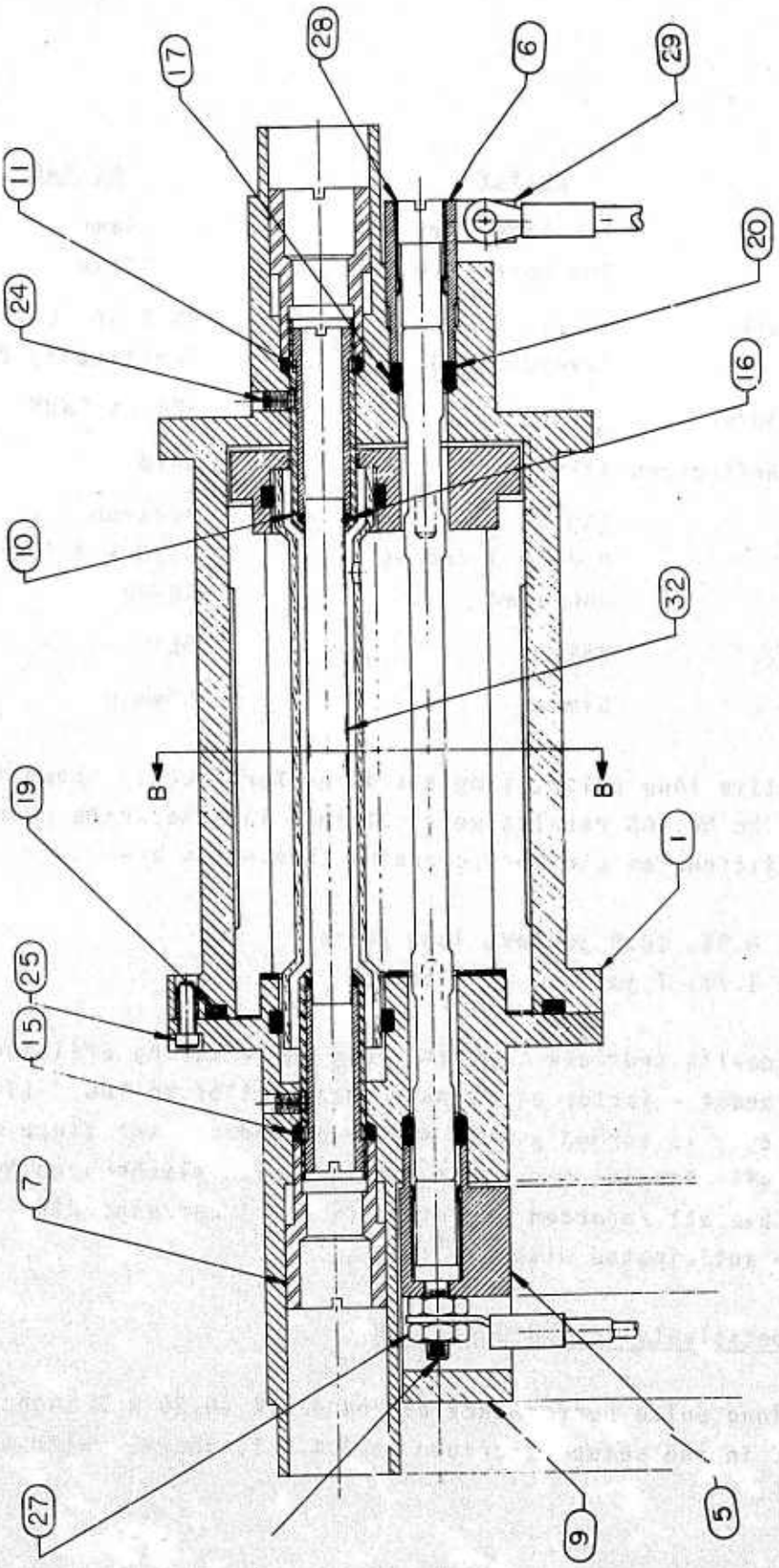

Figure 38. Pogo Pump Cavity

	Er:YLF	Nd:YAG
Pump Lamp:	ILC 1500 Torr Xe 3mm bore, 2.5 inch arc	Same Same
Storage Network:	10 μf, L ≅ o (overdamped)	23.5 μf L=74μh (critically damped)
Flash Pulsewidth:	~20 μs FWHM	~25 μs FWHM
Pump Cavity Reflectors:	Silver	Gold
Rod	479.4 0.25 x 3 inches Uncoated	Airtron 0.25 x 3 inches AR/AR
Output Mirror:	85%	55%
Trigger Mode	Simmer	Simmer

Comparative long pulse, single slot performance is shown in figure 39. The Nd:YAG results were obtained in a separate program. The slope efficiencies and zero crossing thresholds are:

Er:YLF: 0.5%, 10.5 joules, long pulse
Nd:YAG: 1.7%, 7 joules, long pulse.

These results indicate that the long pulse lasing efficiency of Er^{3+}:YLF is about a factor of 3 lower than that of Nd:YAG. Since laser efficiency is strongly pump cavity dependent, and since considerably higher efficiencies have been obtained with flashpumped Nd:YAG (up to 3.3% overall reported in reference 10) corresponding improvements may be anticipated with Er^{3+}:YLF.

4.4.2.2 Repetitively Pulsed Operation

10 Hz long pulse performance of rod 479.4 (0.25 x 3 inches, 7.5% Er) was measured in the setup described in 4.4.2.1, above. With the 10μf

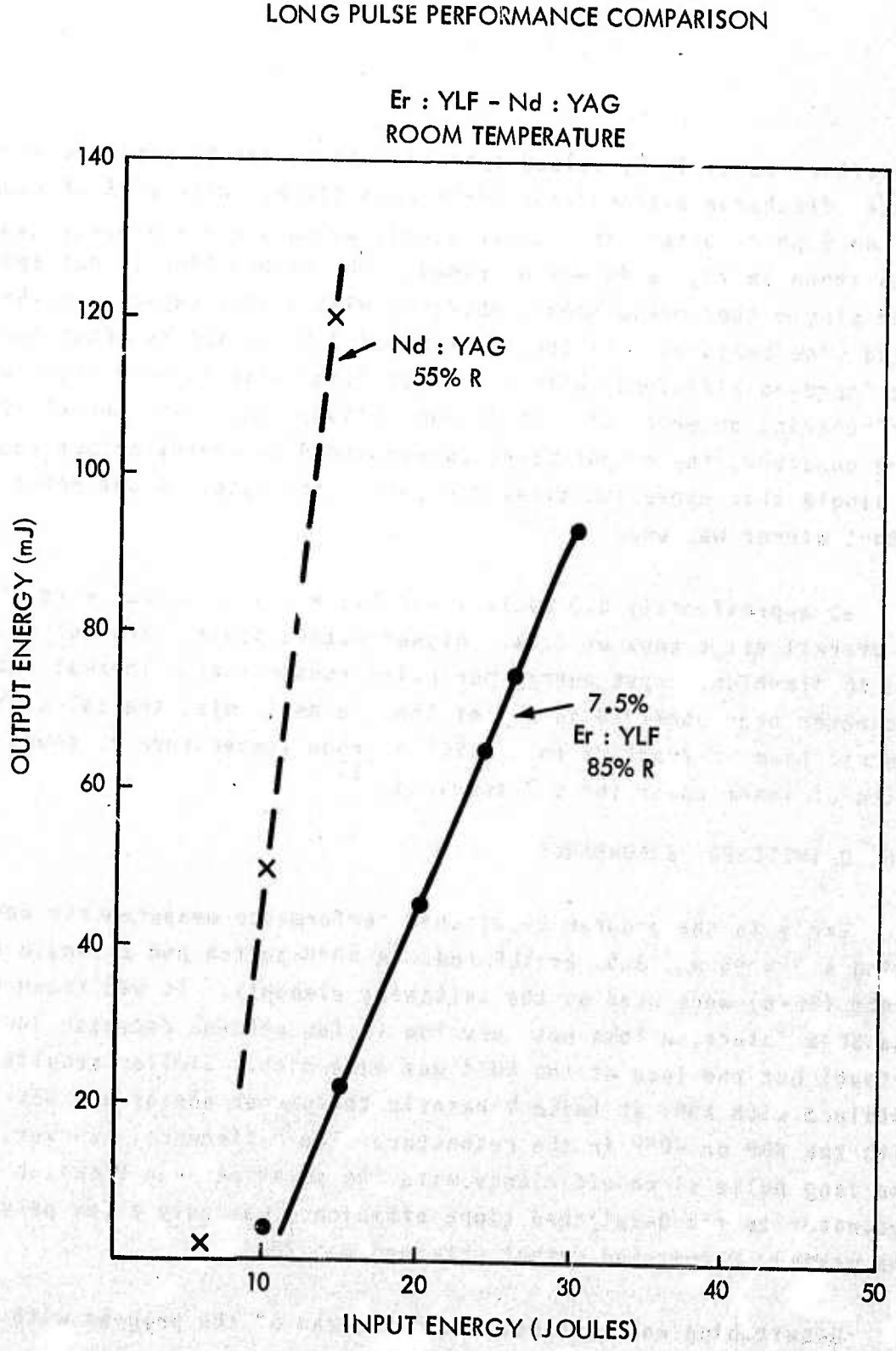

Figure 39. Performance Comparison: Er:YLF-Nd:YAG

capacitor repetitively pulsed operation could not be obtained since the simmer discharge extinguished after each flash. With a 25 μf capacitor and an 8 μh inductor, this power supply anomaly did not occur and the data shown in figure 40 was obtained. The dashed line is extrapolated from single shot measurements obtained with a 10μf capacitor; the solid line measured. As the lifetime of 7.5% Er:YLF is about 50μs, the improved efficiency with a shorter flashpulse is consistent with the behavior observed with 5% Er rods (figure 36). No thermal effects were observed; the output power corresponded to energy output observed in single shot operation times the repetition rate. A one meter radius output mirror was used.

At approximately 370 watts input 1.1 watts of output were obtained, an overall efficiency of 0.3%. Higher output powers were not attempted due to flashlamp input energy per pulse constraints. Thermal fracture has never been observed in any of these experiments; the calculated thermal load at fracture for Er:YLF at room temperature is about 50 watts of laser power for a 3 inch rod.[3]

4.5 Q-SWITCHED PERFORMANCE

Early in the program Q-switched performance measurements were made using a 5 x 45 mm, 3.5% Er:YLF rod. A KD*P switch and a single Brewster plate (SF-6) were used as the switching elements. It was found that the SF-6 insertion loss was very low (a few percent decrease in the output) but the loss of the KD*P was very high. Similar results were obtained with KDP; at twice threshold the output energy was 35% lower with the KDP or KD*P in the resonator. The difference, however, between the long pulse slope efficiency with the polarizer and Q-switch in the resonator to the Q-switched slope efficiency was only a few percent. The maximum Q-switched output obtained was 25mJ.

Q-switching was attempted near the end of the program with

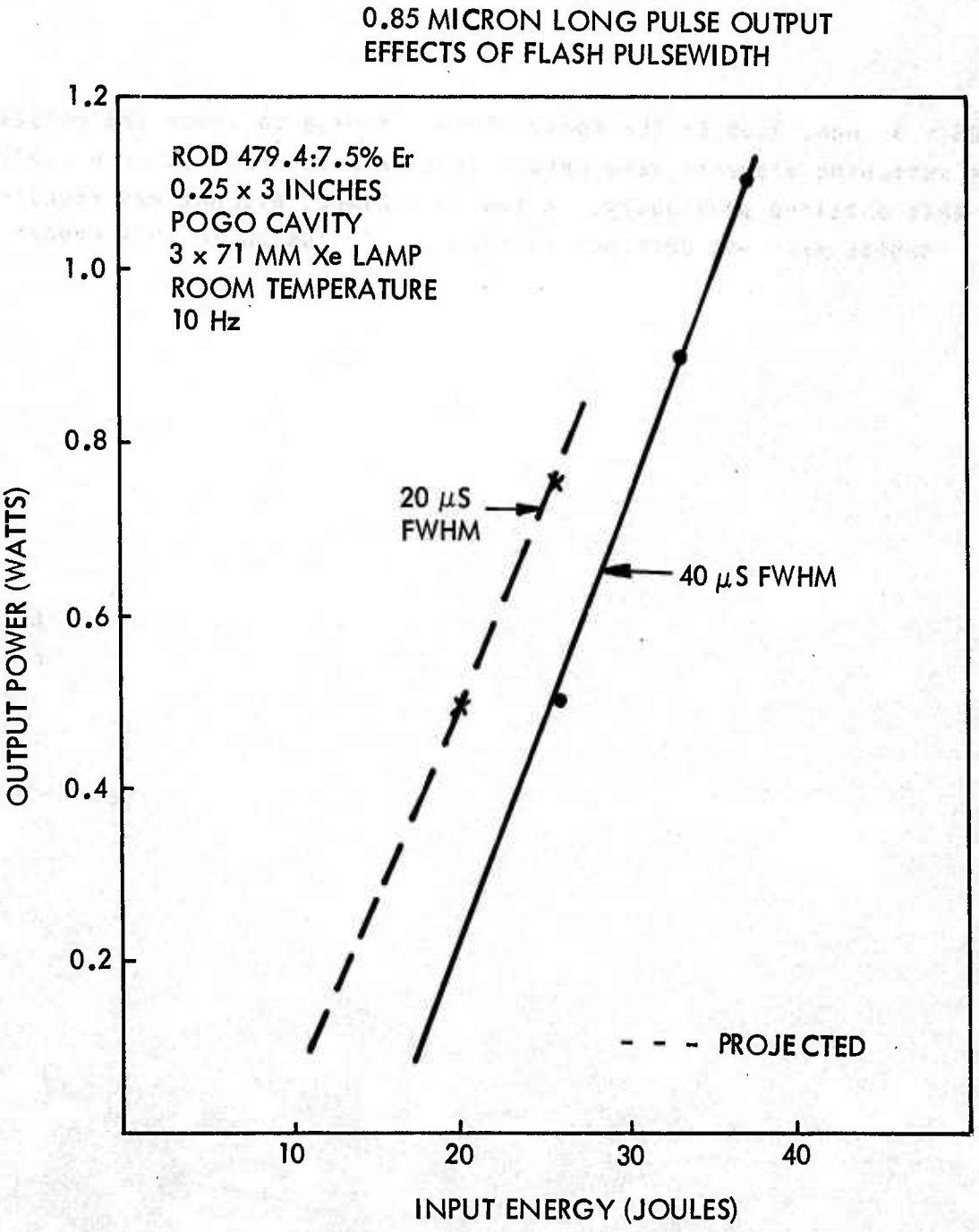

Figure 40. 10 Hz Long Pulse Output Power, 7.5% Er

0.25 x 3 inch, 7.5% Er:YLF rods. Attempts made to lower the losses of the switching elements were unsuccessful and the results were similar to that obtained previously. A low loss $LiNbO_3$ element was received but results were not obtained in time for inclusion in this report.

5.0 CONCLUSIONS AND RECOMMENDATIONS

Growth of large boules of Er:YLF of consistently high quality has been demonstrated on this program after only four "shakedown" runs in an entirely new growth installation. This achievement exemplifies a highly successful technology transfer program from a university laboratory to an industrial installation. The availability of laser rods of consistently high optical and adequate size has resulted in significant improvements in laser performance shown on this program.

This program has demonstrated that under the proper conditions YLF rods with less than 0.5% cm^{-1} scattering loss and much less than a fringe/inch path distortion can be grown on a routine basis. Furthermore the overall boule uniformity has resulted in a rod yield limited by external geometry (there are no cores in this material and the entire boule is usable) and excellent boule to boule reproducibility.

The conditions for growth of high quality material have been described in detail. Suitable pull and rotation rates have been identified and the effects of furnace gradient well documented. Growth of this and most other crystals requires a certain "art"; this has been minimized by diameter control wherein approximately 90% of the growth cycle is entirely automated. However, the initial seeding and "neck down", which must be done manually, have been shown in this program to be critical to the resultant quality of the boule.

Two separate lines of feed purification have been pursued with excellent results. Hydrofluorination of molten $LiYF_4$-$LiErF_4$ (from Research Chemicals YF_3, ErF_3 and Harshaw LiF chips) has reproducibly resulted in high quality material. However, use of fluoride starting materials precludes chemical pre-purification procedures which are

desirable in view of the variability of commercial fluoride feed and the demonstrated effects of feed purification on crystalline quality. (3)

A separate procedure has been developed (at MIT) for synthesis of uniform high purity REF_3 starting from commercial oxides. In this case, the oxide feed is subjected to solvent extraction, converted to a carbonate, then to YF_3 - REF_3. This fluoride feed is then processed in the normal way (i.e., hydrofluorination of molten $LiYF_4$). Results of the only growth run using this feed have been very encouraging; boule 109Y exhibited the lowest scattering ($0.2\%cm^{-1}$) of all the crystals grown on this program.

The technology for growth of high quality YLF crystals has been significantly advanced on this program. Further growth runs with feed prepared from the carbonate process are required to obtain a statistical test of the efficacy of this process for obtaining higher quality material.

Long pulse output powers in excess of 1 watt at 10Hz at a slope efficiency of 0.5% (overall efficiency of 0.3%) were demonstrated at room temperature on this program (0.25 x 3 inch, 7.5% Er). Higher outputs were constrained by flashlamp peak current limitations. At a loading corresponding to an output of 0.12 watt/cm of length the measured beam divergence at 10 Hz was 1.5mr.

Comparative laser measurements show that the efficiency increases linearly with Er concentration from 2-5%. This efficiency increase is anticipated to continue to at least 10% Er with flash pulsewidths shorter than the fluorescence lifetime. Substantilly more Q-switched data is required to define the performance of this material. Q-switched output energies corresponding to one-half the long pulse output was demonstrated. However, efficiency was low due to the high insertion loss of the KD*P and KDP elements available.

The major problem encountered during this program was the very rapid degradation of pump lamps when operated with a pulse width less than the fluorescence lifetime. This is due to a peak current limitation of flashlamps which is determined by the electrode diameter only and is not associated with normal flashlamp aging. The increasing laser efficiency with Er^{3+} concentration is well documented in this report. But as the Er^{3+} concentration increases the upper level lifetime rapidly decreases. Maintaining a flash pulse shorter than the fluorescence lifetime severely limits the available input energy. For example for 3 inch rods with a 50μs lifetime the maximum input energy was approximately 30 joules. There are several alternatives available for obtaining higher average power in this material at room temperature. They are:

a. Higher repetition rates

Since the peak current limitation under these conditions is very far below the explosion energy limit (a 3 x 70 lamp with a 25μs pulse has an explosion energy of about 200 joules, but a maximum current of 500 amps or about 30 joules), higher average power with long lamp life can be obtained at higher repetition rates at a reduced energy per pulse. However, the overall efficiency will be somewhat lower for the same average power output depending upon how close to threshold one operates. For this program measurements were restricted to 10Hz.

b. Larger bore lamps

As the peak current increases with the square of the electrode diameter this approach has obvious merit. In particular it appears most useful for pumping rods in close coupled cavities or in other laser material configurations where the problems of imaging a source larger than the active material can be avoided. The use of multiple lamps provides another means of improvement. Alternatively, the use of dye laser flashlamps, particularly coaxial lamps appears

attractive. Such lamps can dissipate much higher peak currents and YLF has been shown to be immune to flashlamp induced damage from such discharges [11]. Furthermore, with 1-10μs flashpulses much higher Er^{3+} concentrations can be utilized effectively; for some applications Q-switching may not be required (the laser emission will persist only during lamp discharge); and dye laser lamps are better matched spectrally to the Er:YLF pump bands.

c. Sensitization

The route explored on this program for improved efficiency can be thought of as "self-sensitization". Improved optical coupling was obtained by increasing the active density. Sensitization by other rare earth runs has not been explored on this program but would be attractive provided the energy transfer rate was much faster than the upper level lifetime. Furthermore the sensitizing ion(s) must be transparent to .85μ radiation.

d. Selective Emitters

In Nd materials pumping efficiency is enhanced by line emission of Xe and Kr discharges in the 0.7 - 1 micron region. In a water cooled Er:YLF laser, useful pump bands extend from 0.25 - 0.55 microns a region of continuum emission from Xe lamps. Xe discharges in this region are optically thin and emission can be enhanced by additives. Hg looks particularly attractive as a Xe lamp additive. The strong emission lines at 0.254, 0.365, .405, and 0.546 microns well match Er absorption lines.

e. Larger Active Volumes

Unlike Nd:YAG the size of Er:YLF rods is not constrained by cores; virtually the entire boule is useful. This suggests the use of larger rods or structures which lend themselves to larger material

volumes (Face Pumped Laser, for example) for higher energies per pulse and higher average powers.

In summary Er:YLF provides a source of very high radiance with moderate output power and efficiency. The efficiency of this material in its present state of development is about a factor of 3 lower than that of Nd:YAG. The most direct route to performance improvement at room temperature appears to be use of "unconventional" pumping techniques (dye laser lamps or selective emitters in the blue-uv) and pumping geometries (larger rods or Face Pumped Laser). The improved efficiency with Er concentration together with concentration quenching of the upper loss level lead to an optimum Er concentration of between 5-7% in 0.25 x 3 inch rods at the 1 watt level in conventional laser pump cavities. It is emphasized that the calculated thermal figure of merit [3] of this material indicates that a 0.25 x 3 inch Er:YLF rod is capable of 10 watts output at approximately 20% of the fracture loading.

REFERENCES

1. E.P. Chicklis, C.S. Naiman and A. Linz, "Stimulated Emission at 0.85 μm in Er:YLF," Digest of Tech. Papers, VII International Quantum Electronics Conf., p 17, May 1972.

2. E.P. Chicklis, R.C. Folweiler, C.S. Naiman, D.R. Gabbe, A. Linz, and H.P. Jenssen, "Development of Multiply Sensitizer Ho:YLF as a Laser Material", ECOM-73-0066F, Oct. 1974.

3. E.P. Chicklis, R.C. Folweiler, C.S. Naiman, et al. "0.85 Micron Solid State Laser Material Evaluation." AFAL-TR-73-94, PART III, June 1974.

4. D. Findlay and R.A. Clay, Phys Letts. 20, 3, pp 277-278 (1966).

5. D.W. Goodwin, Phys. Lett. 24A, 5, pp 283-4 (1967).

6. E.P. Chicklis, R.C. Folweiler, C.W. Naiman, D.R. Gabbe, and A. Linz, "Er:YLF Laser Development", AFAL-TR-75-69, PART I, April 1, 1975.

7. E.P. Chicklis, R.C. Folweiler, C.S. Naiman, et al, "0.85 Micron Solid State Laser Material Evaluation", AFAL-TR-73-94, PART II, OCT. 1973.

8. ILC Data Sheet

9. In αβYLF where most of the pumping is due to Er absorption, pump uniformity for 3 mm rods with 50% Er has been found to be quite good, M. Perlmutter, MIT/CPL, private communication.

10. L. Noble et al, "Optical Pumps For Lasers" ECOM-0239-F, OCT. 1973.

11. H.P. Jenssen, D. Castleberry, D.R. Gabbe, and A. Linz, IEEE J. Quantum Electronics QE-9, 665 (1973).

☆ U. S. GOVERNMENT PRINTING OFFICE: 1976 — 657-030/577